

**AD719840**

**71-0528**

**GEOPHYSICAL INSTITUTE**

**of the**

**UNIVERSITY OF ALASKA**

**Final Report**

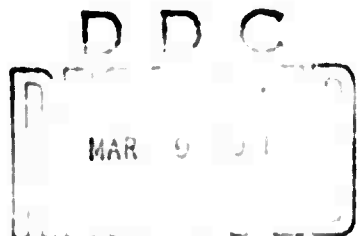
**CRUSTAL DEFORMATION RELEASE,  
FAILURE AND TILTS IN ALASKA**

**by**

**Edward Berg**

**Affid Contract F-44620-70-C-0031**

**January 1971.**



**Approved by:**

**C. R. Berg**

**Geophysical Institute**

**Approved by:**

**Keith R. Mather  
Director  
Geophysical Institute**

1. This document has been approved for public release and sale; its distribution is unlimited.

**NATIONAL TECHNICAL  
INFORMATION SERVICE  
Springfield, Va. 22151**

# **DISCLAIMER NOTICE**

**THIS DOCUMENT IS THE BEST  
QUALITY AVAILABLE.**

**COPY FURNISHED CONTAINED  
A SIGNIFICANT NUMBER OF  
PAGES WHICH DO NOT  
REPRODUCE LEGIBLY.**

**GEOPHYSICAL INSTITUTE  
of the  
UNIVERSITY OF ALASKA**

**AFOSR Contract No. F-44620-70-C-0031**

**Project Title: Crustal Deformation Release, Failure  
and Tilts in Alaska**

**ARPA Order No. 292, Amd. 75**

**ARPA Program Code No. OF10**

**Starting Date: 1 November, 1969**

**Termination Date: 31 October, 1970**

**Amount of Contract: \$80,000**

**Project Scientist: Dr. Eduard Berg  
Geophysical Institute  
University of Alaska**

**Telephone Number: 907: 479-7373**

## TABLE OF CONTENTS

	Page
TABLE OF CONTENTS	iii
PERSONNEL	iv
ACKNOWLEDGMENTS	v
ABSTRACT	vi
LARGE APERTURE TELEMETRY SYSTEM FOR CENTRAL ALASKA AND FAIRBANKS MICRO-EARTHQUAKE NETWORK	1
BOREHOLE LONG-PERIOD INSTRUMENTATION	3
THE EFFECT OF BAROMETRIC PRESSURE VARIATION ON THE "U.S.O." LONG-PERIOD SEISMOMETER-CONTRIBUTION BY EDUARD BERG AND RONALD RASMUSSEN (FEBRUARY, 1970)	5
CRUSTAL MORPHOLOGY OF CENTRAL ALASKA-CONTRIBUTION BY JOHN DAVIES (M.S. THESIS, MAY, 1970)	7
TILOTS PRECEDING EARTHQUAKES-CONTRIBUTION BY EDUARD BERG	8
TILOTS ASSOCIATED WITH SMALL AND MEDIUM SIZE EARTHQUAKES- CONTRIBUTION BY EDUARD BERG AND HANS PULPAN (NOVEMBER, 1970)	9
DEFORMATION AND FAILURE IN AN EARTHQUAKE ZONE-CONTRIBUTION BY EDUARD BERG AND DATA ANALYSIS BY NIKI BLOOM.	28
a.) Earthquake Statistics and Stress	28
b.) Deformation Prior to Failure	29
c.) Dilatancy and Vp/Vs Ratios	30
d.) Results of Micro-Earthquake Analysis in the Fairbanks Area.	31
LIST OF PUBLICATIONS ACKNOWLEDGING AFOSR SUPPORT	33
REFERENCES	34
LIST OF FIGURES	38

## PERSONNEL

The program of integrated research described in these pages would not have been possible without the interest, dedication and professional competence of every member of the seismological laboratory. The principal investigator wishes to express his gratitude and thanks to all, and looks forward to the achievements that the continuing cooperation will bring.

Dr. Hans Pulpan, Assistant Professor

Larry Gedney, Assistant Geophysicist

Douglas VanWormer, Assistant Geophysicist

John Davies, Senior Research Assistant

William Lutschak, Senior Research Assistant

Niki Bloom, Research Assistant

Ronald Rasmussen, Engineer

Orwin Westwick, Engineering Aide

Linda Petz, Data Analyst

#### ACKNOWLEDGMENTS

We want to express our thanks and appreciation to Mr. William Best, Chief, Geophysics Division, AFOSR, for the continued interest and support which made this research program possible. We acknowledge the efficient help of the Alaska Air Command, RCA, and the Army (Fort Wainwright), for establishment and continued maintenance of the communication links of the telemetry system. Sincere thanks go to the NASA STADAN station Director, Ed Eisele, for permission to operate and maintain the Gilmore (GLM) borehole station, for the help given on numerous occasions and for permission to use a data link. Thanks also are expressed to Judge Hepp, for the generous permission to install a short-period seismometer (HPP) on his private property and the continuous use of power to operate the station.

Finally we would like to express appreciation to Mr. Howard Butler, Chief, U.S.C. & G.S., Palmer Tsunami Warning Network and to Mr. Jack Townshend of the College Observatory, for providing records and other useful information for the present program.

## ABSTRACT

This report covers the effort during a one year period from the end of 1969 to the end of 1970, supported by AFOSR. The main purpose of the contract was to gain insight into the crustal failure mechanism and the associated source phenomenon in Alaska. This effort includes the operation of the short-period telemetry network and the three long-period borehole installations used for the measurements of crustal tilts.

Through the telemetry system there is now on hand an almost complete record on the seismicity of Central Alaska, covering a total of four years, and of much higher accuracy than was hitherto available.

The operation of the borehole long-period seismometer has revealed tilts associated with earthquakes as small as magnitude 3, which are consistent with the tectonic stress axis, but do not seem to conform to elastic fault dislocation models. Tilt amplitude reductions with distance R is of the form  $A$  (in sec of arc) =  $10^{M-4.1} \times R^{-1}$  and velocities of tilt propagation are in the range 2.1 to 2.8 km/sec for near earthquakes (focal point to station) and up to 3.3 km/sec for teleseisms. In view of the discrepancies with elastic dislocation theory, a surface or crustal type propagation is suggested.

Analysis of literature suggests that Russian observations of the  $V_p/V_s$  ratio, diminishing by about 0.1 prior to larger earthquakes, can be explained by the decrease in  $V_p/V_s$  ratio due to micro-fracturing (observed in the laboratory) and theoretical as well as experimental work on  $V_p/V_s$  changes as a function of porosity. However, so far we have been unable to observe such effects in the Fairbanks, Alaska, micro-earthquake area.

Finally the exponential increase of deformation (strain, tilt, strain release) often observed prior to large earthquakes can be explained through microscopic dislocation theory.

In the following, published articles, reports, etc. are given as abstracts; other work is rendered in more detail.

LARGE APERTURE TELEMETRY SYSTEM FOR CENTRAL ALASKA  
AND FAIRBANKS MICRO-EARTHQUAKE NETWORK.

The telemetry system was planned in 1965. The first station operated in the winter of 1966-67. The number of short-period vertical high-gain stations has increased steadily since. Also included are three borehole installations, including short-period and 15 sec long-period 3-component seismometers with displacement transducers.

The geographical coordinates of the stations were selected so as to cover the regions of highest seismicity in the Alaskan interior, the area of active volcanoes adjacent to Cook Inlet (the oil fields), and the Alaska Peninsula (Figure 1). The micro-earthquake network includes the area of the Fairbanks, June 1967 M=6 earthquake epicenter and the aftershock zone (Figure 2). The tripartite borehole net was installed to cover the interior and to study crustal tilts associated with local and distant earthquakes.

All vertical short-period seismometers are recorded at the Geophysical Institute telemetry terminal on 16 mm film (Develocorder) with the exception of a seismometer in the building itself. The record of this seismometer is a heat sensitive one (Helicorder). The remoteness of many stations from settlements and traffic allows operation at very high gains and location of earthquakes of magnitude 1.5 to 2.0 within the network. The equipment has been described in earlier reports by Berg and others (July 1967) and Berg (January 1970).

The five oldest stations in the network have been recalibrated during the summer of this contract period by John Davies, Ron Rasmussen, and Douglas VanWormer. They are: BIG (2.4 million), SVW (2.8 million),

TNN (1.1 million), BLR (6.5 million), and SCM (2.1 million, at 10 Hz). The numbers in parenthesis give the present magnification at 5 Hz as seen on the film viewer. The following Table lists the presently operating stations (see also Figure 1 and Figure 2).

**UNIVERSITY OF ALASKA  
SEISMIC TELEMETRY NETWORK**

**SP VERTICAL ONLY**

SVW	61°06.9'	155°35.9'	
BIG	59°23.36'	151°12.98'	562m
TNN	65°15.4'N	151°54.7'W	504m
SCM	61°50.00'	147°19.66'	1020m
BLR	63°30.10'	145°50.72'	809m
MCB	64°43.70'	147°12.61'	213m
MIN	64°52.34'	147°49.68'	160m
PJD	65°02.065'	147°30.55'	740m
BRH	64°51.09'	147°38.42'	330m
HPP	64°47.43'	147°57.55'	170m
LV	64°51.62'	147°50.91'	180m

**BOREHOLE**

MCK	63°44.02'	148°55.95'	610m (ground surface)
P/X	62°58.19'	145°28.12'	1034m (ground surface)
GLM (pre 'm)	64°59.24'	147°23.34'	722m (ground surface)

## BOREHOLE LONG-PERIOD (LP) INSTRUMENTATION

The long-period seismometers of the Lamont-lunar-ocean-bottom type (with displacement transducers) have been operating through most of the contract period. Several weeks of down-time occurred in connection with the move from the old (Chapman) to the new (Elvey) Geophysical Institute building. The unavoidable dismantling and reinstallation of the seismic telemetry terminal, and the Institute's microwave link took several weeks.

The interface problems between the borehole electronics and the recording telemetry terminal have been solved in the following manner:

### Stations GLM and MCK:

The demodulator output signals are amplified 25 times at the borehole. The DC offset of the demodulator output is compensated by using the automatic feedback signal at the second input of the x 25 differential amplifier. The long-period response does not suffer considerably by this arrangement. The amplified signal is then transmitted over the telemetry link. Tilt signals from the feedback amplifier output are amplified 10 times before transmission.

### Station PAX:

This station seems to be very stable tectonically, so that the automatic feedback was removed; this in turn gives a 30db higher DC output at the demodulators for long-term tilts as compared to the stations with automatic feedback. So far the seismic signals have not been amplified at the PAX station before transmission. This has proven to be excellent in the case of the magnitude 8 New Guinea earthquake on January 10, 1971, where tilt offsets clearly are visible on the

Helicorder records (as well as on the slow-speed and filtered tilt records). However, to maintain a near-center position of the transducers, a DC voltage has been applied to the feedback line. Since 24 June, 1970 (when the fixed DC was installed in PAX), a total of three adjustments only have been necessary (25 August, 4 September, and 10 November) to keep the demodulator output within the telemetry channel until mid January 1971 ( $\pm$  2.5 volt or roughly 1/3 of a second of arc in tilt).

In all stations the circuitry for automatic releveling has been removed, and releveling is done by inserting the appropriate circuit cards when necessary. The reason for removing the relevel circuitry was to avoid releveling during earthquakes. This situation had occurred several times and prevented the recording of tilts associated with those earthquakes. This was especially detrimental during the M = 6.7 to 7 earthquake near Yakataga on April 16, 1970. Tilts in the direction of the epicentral area had been recorded during the three days prior to the earthquake at PAX and GLM, and apparently continued in that direction during the earthquake, but the total amount is unknown because all three stations leveled the instrument platform automatically during the earthquake.

Finally new paper chart recorders (25 cm wide) obtained from other Geophysical Institute funds have been installed for tilt recordings. Paper speed is 2.5 cm/hour and sensitivity to tilt under normal recording conditions is about 1 mm/msec arc for PAX and about 1 mm/3 msec arc for GLM. However, the sensitivity to extremely rapid tilts, as occurring during earthquakes, is considerably higher on the long-period records. For comparison, refer to the contribution by Berg and Pulpan on tilts associated with earthquakes.

THE EFFECT OF BAROMETRIC PRESSURE VARIATION  
ON THE "U.S.O." LONG-PERIOD SEISMOMETER

Contribution by

Eduard Berg and Ronald Rasmussen

(February 1970)

ABSTRACT

"The particular manner of mechanical construction of the long-period U.S.O. package is responsible for the pressure sensitivity of the LP-X component. The effect seems to be linear with pressure for periods larger than the seismometer period and short compared to the feedback signal time constant. Under the particular setting of the Gilmore (GLM) installation, a pressure-induced displacement of the x component is  $\frac{\Delta x}{\Delta p} = \frac{-13.8 \text{ mm}}{\text{u bar}}$  (without feedback).

Since the pressure-induced displacements are considered as very undesirable noise for the instrument as either long-period seismometer or as tilt meter the borehole was pressure-sealed and the effect removed. Records are presented to demonstrate the effect."

The effect was fully realized when the tilts (obtained by recording the feedback signal) for the three borehole instruments were plotted together with the barometric pressure variation (obtained from the Weather Bureau, Fairbanks International Airport) Figure 23 represents the data. For further details refer to Berg and Rasmussen (February 1970).

The GLM borehole was pressure sealed on December 6, 1969, the PAX borehole on 22 February, 1970, and MCK in August 1970. The seal is of a well-head type, machined and prepared in the Geophysical Institute to fit the 12 inch inside diameter of the borehole casing and the individual package cables. It consists of two half-inch thick aluminum plates and sandwiched rubber. Upon installation, the rubber was lubricated with liquid rubber and compressed between the two plates and pressed against casing and cables. The additional liquid rubber sealed the sandwich against the casing and cable. To take care of any small leaks which might occur along the screws, about two quarts of "Asphalt Lap Cement" were simply poured on top of the seal. Time has shown that these seals are effective and that no pressure variation is transmitted to the instrument through the air column.

## CRUSTAL MORPHOLOGY OF CENTRAL ALASKA

Contribution by

John N. Davies (May 1970)

This M.S. Thesis was completed during the present contract period under the supervision of the principal investigator. The work was also financed through a National Science Foundation grant, and drew heavily on data from the telemetry network.

### ABSTRACT

"Earthquake-generated waves were used to calculate dips of the crust-mantle interface below station pairs using the apparent velocities from the telemetry network, the U.S.C. & G.S. Tsunami Warning System and a number of temporary field sites. Apparent mantle P-wave velocities ranged from  $7.0 \pm 0.4$  to  $10.6 \pm 0.7$  km/sec. Crustal thicknesses were found to be 34 km under Fairbanks, 37 to 47 km in different locations under the Alaska Range, 24 to 36 km in the Kuskokwim, Susitna, and Copper River Valleys, and also 35 to 42 km in the Palmer area. The focal point distribution of the earthquakes used in this study suggest that the Cook Inlet-Susitna topographic low is a continuation of the Aleutian Arc zone of subsidence of the Pacific plate."

## TILTS PRECEDING EARTHQUAKES

Forerunning tilts are separable into those of extended duration (of the order of one year) and those preceding the earthquake by a few days or hours. So far we have been able to observe only one occasion of simultaneous tilts at the station PAX and GLM. The earthquake occurred in the Gulf of Alaska near Yakataga on 16 April, 1970, at 0533:17.5 GMT and 59.8N 142.6W (U.S.C. & G.S. preliminary epicenter determination) and had a magnitude of 6.5 (PAS), 6.5-7.0 (BRK) and 6.2 ML(C.G.S.). This epicenter is in line with the stations GLM-PAX at a distance of 400 km from PAX and 650 km from GLM. The tilts at both stations were in the direction of the epicenter and preceded the earthquake by 3 days. The total tilt amplitudes were approximately 0.3 sec arc at GLM and 0.1 sec arc at PAX. They closely agree with tilt amplitudes reported in the literature of 30 and 100 msec arc (Sassa and Nishimura, 1951; Nishimura, 1958). The direction of tilt prior to the earthquake seems to correlate with that during the earthquake. Unfortunately, however, the tilt amplitude during the earthquake is not available because the instruments were triggered by the large amplitudes and leveled automatically. Figures 24 and 25 show the tilts for PAX and GLM during the period preceding the earthquake. Also, attention is drawn to the 40 msec arc so-called "S" loop occurring some 20 hours prior to the final failure. Russian investigators (Karmaleeva, 1960, 1962) successfully used these "tilt storms" for earthquake prediction. A similar loop also has been observed at GLM some hours prior to a local Fairbanks earthquake of magnitude 3.7 to 4 on November 24, 1970. This particular earthquake showed also associated crustal deformation as those reported in the following section.

TILTS ASSOCIATED WITH SMALL  
AND MEDIUM SIZE EARTHQUAKES

Contribution by

Eduard Berg and Hans Pulpan (November 1970)

This paper also was supported by an AEC contract and presented by Eduard Berg at the Geophysical Institute, University of Tokyo, Japan on 19 December, 1970.

SUMMARY

Tilt observations from nearby local earthquakes in the magnitude range from 3 to 5 and larger teleseisms show an amplitude reduction with epicentral distance R of the form  $A$  (in sec/arc) =  $10^{R^{4.1}} \times R^{-1}$ . The result is compared to static elastic dislocation models. Velocities of the tilt propagation are in the range 2.1 to 2.8 km/sec for near earthquakes (focal point to station), and up to 3.3 km/sec for teleseisms. In view of the discrepancies between strain and tilt observations and static elastic dislocation theory, the tilt reduction with distance, and the propagation velocities, the strain and tilt steps are viewed as a surface-type propagation phenomenon.

The earthquake-associated tilts and first motions imply a south-southeast to north-northwest compression along the northern edge of the Tanana Basin. Earthquake locations and depths indicate active faults south of Fairbanks along the northern edge of a gravity low, along the Chatanika River, and on the northern extension of the Minto fault. The first two of these faults have not been known before.

## INTRODUCTION

The problem of understanding crustal failure is to relate measurable quantities to the stress state of the crustal rock and, if possible, to its time history. This can be achieved relatively easily in the laboratory, but application to earthquake seismology is vastly more complex. Comprehensive laboratory experiments relating to stress, strain, and microfracturing, and their interpretation have been performed by a number of authors - Mogi, Scholz, Brace, and Byerlee to name a few - directly interested in crustal rocks, and applied to an earthquake zone (Berg, 1968) relating stress to earthquake statistics. Low "b" values of the Gutenberg-Richter relation  $\log N = a + b(8-M)$  are associated with foreshocks and in relation with the magnitude of the main shock (Berg, 1968).

The final failure is also preceded by a rapidly increasing deformation. In an earthquake area such a preceding deformation can be measured in the field by strain seismographs, tilt meters, or geodetic surveys (Carder, 1945; McGinnis, 1963; Berg, 1966; Rothé, 1968; Gough and Gough, 1969 and 1970), and is known to be accompanied by changes in electric resistivity, seismic velocity, velocity ratios, and the magnetic field. Seismic strain release sometimes shows this rapid increase prior to failure.

During the final rapid failure (fracture) the stored elastic energy is transformed into separation, plastic, kinetic, as well as heat energy. The dislocation associated with the (crustal) earthquake produces a strain and tilt field. This deformation field can be observed with modern high sensitivity strain and tilt meters at large distances, if

the magnitude of the earthquake is sufficiently large. The question of transient and residual deformation of the earth's crust has seen renewed interest due to studies associating earthquakes with large underground nuclear explosions (Ryall and others, 1969), loading effects of large artificial water bodies, and crustal failure due to lowering of the rock strength due to fluid injection (Healy and others, 1968). Pre-existing tectonic stress level and the additional induced strain will be responsible for triggering of subsequent earthquakes, but to date little is understood about these stress levels and the failure-induced strains associated with relatively small earthquakes.

In this paper, the amplitude-distance-magnitude relation of observed tilt steps and their propagation velocities are reported and compared to results from other authors' mathematical models based on static elastic dislocation theory.

## INSTRUMENTS

In the fall of 1968 and the summer of 1969 a tripartite tilt network was installed in Central Alaska. The stations are located at Gilmore (GLM), McKinley (MCK), and Paxson (PAX). Station locations and altitudes are as follows:

MCK	$63^{\circ} 44.02' N$	$148^{\circ} 55.95' W$	610 m (ground surface)
PAX	$62^{\circ} 58.19' N$	$145^{\circ} 28.12' W$	1034 m (ground surface)
GLM	$64^{\circ} 59.24' N$	$147^{\circ} 23.34' W$	722 m (ground surface) (Preliminary)

Figures 1 and 2 show the location of the network in Central Alaska along with the short-period telemetry stations.

Instruments used are the Lamont-type horizontal pendulums ( $T_0 = 15$  sec) with a 30 db feedback loop and capacity type transducer. They are contained in a 10 inch diameter borehole package and installed in 12 inch inside diameter steel casing at depth of 15 feet at GLM, 28 feet at MCK, and 38 feet at PAX. The choice of the three sites was dictated, among other factors, by available power and communications. All data are telemetered by standard IRIG-FM channels 1 through 7 over phone circuits and recorded at the Geophysical Institute of the University of Alaska.

At the free pendulum period of 15 seconds the equivalent pendulum length is 57.3 m. A  $1\mu$  change in the transducer position of a horizontal pendulum of length 57.3 m corresponds, therefore, to a tilt of  $1.745 \cdot 10^{-8}$  radians (in a direction perpendicular to the plane sustained by the vertical and the axis of rotation of the pendulum).

Since  $1 \text{ sec arc} = 4.85 \times 10^{-6}$  radians, a 15 sec pendulum has a sensitivity to tilt of  $278 \mu/\text{sec arc}$ . This sensitivity is reduced by the amount of feedback applied. At GLM and MCK a feedback of 30 db

(31.6) is applied after a filter with a RC time constant of 6000 sec. With the transducer sensitivity of  $25 \text{ mV}/\mu$ , the 30 db feedback and a  $\times 10$  amplifier at the station, a total sensitivity to tilt of  $2.2 \text{ V/sec}$  arc is obtained for variations with longer duration than the feedback filter time constant. The telemeter link has 1:1 gain. The chart recorder is now operating at  $5 \text{ mV/mm}$  and  $25 \text{ mm/hour}$ .

The PAX station proved stable enough, so that the feedback circuit could be removed and a higher sensitivity obtained. Also, for the Rampart earthquake tilts, use has been made of the standard horizontal Wood-Anderson seismographs, operated by the U.S. Coast and Geodetic Survey on the College campus of the University of Alaska.

#### TILTS ASSOCIATED WITH EARTHQUAKES

Earthquake-associated tilts have been reported in the literature from various continents and using a variety of instrumentation, mostly for shocks with  $M > 5$ . Recording of tilts associated with low-magnitude earthquakes is relevant to the problem of focal mechanism, permanent crustal deformation and its propagation. In Russia and Japan (Karmaleeva 1960 and 1962; Hagiwara, 1969), tilts also have been used successfully to predict impending earthquakes.

However, often the reliability of tilts as recorded on horizontal seismometers has been questioned, mainly because recorded amplitudes have been large compared to theoretical calculations. Besides liquid level tilt meters, one might either use the direct optical recordings from the Wood-Anderson torsion seismometers, the Verbaandert-Melchior all-quartz pendulums (Verbaandert and Melchior, 1960) or the long-period horizontal seismometers with high sensitivity displacement transducers, as installed in the three borehole packages.

Hagiwara (1969) reports on differences between instruments: "We often observed sharp change in the tilting a few hours before the occurrence of earthquakes of about magnitude 5. Such short range changes just before a large earthquake were clearly observed with the water tube tilt meter, but they were not detectable by the pendulum type tilt meter. The reason why the water tube tilt meter indicates changes and the pendulum tilt meter does not is not entirely clear, but one solution will be proposed. For the long range changes in tilt, observational results of the water tube tilt meters and the pendulum tilt meters coincide well with one another".

The block-type structure of the earth's crust also affects and complicates the tilt recordings locally. Studies report on significant differences at stations spaced only a few hundred meters apart (Ozawa, 1963; Hagiwara, 1938).

The question, therefore, arises a.) whether the permanent displacements observed (or calculated) at the transducers of horizontal pendulums are real tilts, or effects generated in the instruments themselves, such as creep in the hinges (etc.) during the ground vibration of the earthquakes; and b.) how do observations relate to theoretical results from static elastic dislocation theory, the only one available at this moment. A number of literature reports will therefore, be compared with the recordings in Alaska.

#### THEORETICAL RESULTS

In order to relate the observed tilts, reported in the later section, to theoretical work, the essential points of the static elastic dislocation theory are exposed in this section.

A number of theoretical papers gradually extended the concept of a Volterra dislocation, generated during an earthquake, from simple half space-vertical fault plane, to spherical earth-inclined plane solutions (Chinnery, 1961; Maruyama, 1964; Press, 1965; Singh and Ben-Menahem, 1969; Ben-Menahem and others 1969 and 1970), and with the advent of electronic computers many numerical calculations of the resulting strain, stress, and tilt fields could be carried out. All of these theories have evolved from a static, elastic dislocation model. The theoretical reduction of tilt and strain fields with distance R from the source varies from  $R^{-1}$  to  $R^{-6}$ , (Maruyama, 1964; Press, 1965; Ben-Menahem and others 1969, 1970). This variation depends strongly on the particular type of dislocation (strike slip or dip slip fault) and the orientation of the observing line with respect to the fault, but rather weakly on Poisson's ratio. Ben-Menahem and others (1969) found it hard to accept a simple universal exponent for all faults, strains, and azimuths, such as -1.5 found by Wideman and Major (1967). They note, however, that certain sources "transmit" strains in certain directions with relatively low loss (low exponent value). These are certainly the most obviously recorded cases, whereas those with faster reduction are not so easily found at larger distances. It will be shown in the section on observations, that the experimental tilt data, similarly, seem to indicate a rather narrow possible range of exponents for the amplitude-distance relation.

Ben-Menahem and others also comment (in both papers, 1969 and 1970) on the differences between half space and spherical solutions. These differences seem to be small for distances less than  $20^\circ$  to  $30^\circ$ . For most of the small earthquakes in the magnitude range  $3 < M < 5.7$  and at distances up to several fault lengths, one might, therefore, use Press's

half space model (1965). This model assumes vertical fault plane, pure strike slip or pure dip slip motion for a given fault length-depth ratio and two different fault length-slip ratios. Press's formulas for tilt in the case of dip slip motion result in the following approximations at large distance along the axis (using the notation of Press):

On  $x_1$  axis:

(strike of fault)

tilt in  $x_1$  direction = 0

$$\text{tilt in } x_2 \text{ direction} = \frac{U_3}{2\pi} \frac{4L(D-d)}{D \cdot d} \cdot \frac{1}{x_1} \text{ for } x_1 \gg L, D, d$$

On  $x_2$  axis:

tilt in  $x_1$  direction = 0

$$\text{tilt in } x_2 \text{ direction} = \frac{U_3}{2\pi} \frac{2L}{x_2^5} L^2 (D-d) + 3(D^3 - d^3)$$

for  $x_2^2 \gg L^2, D^2$ , and  $d^2$

The dependence on distance is of the form  $R^{-1}$  along the direction of the strike of the fault and  $R^{-5}$  perpendicular to it. The very strong dependence on fault length ( $2L$ ), depth of burial  $d$  (upper edge of fault), or  $D$  (lower edge), and fault depths ( $D-d$ ) is evident. As mentioned by Ben-Menahem and others (1970) also, the dip slip fault gives rise to an amplitude dependence of tilt on depth like  $D \cdot d$ .

These reduction ratios are obtained from Press's numerical output for distances larger than 3 fault lengths. In the strike slip case tilt amplitude diminishes with distances as  $R^{-2.5}$  (on the computer outputs). The tilt directions and tilt amount (presented in Figure 3) have been obtained from Press's calculations for a vertical surface fault, with

a depth of 1/2 its length and a displacement of  $\frac{4}{3} \times 10^{-4}$  its length.

The tilt directions and amplitudes are later compared to those recorded in the Fairbanks area. Similarly, tilt directions can easily be seen by drawing perpendiculars to the lines of equal vertical displacements in Maruyama's (1964) figures of surface displacements and the resulting tilt directions resemble those obtained by Press.

#### TILT OBSERVATIONS

In this section observations of tilt steps and the amplitude-distance-magnitude relationship is elaborated. Wideman and Major (1967) similarly reported on the strain steps observed from a number of earthquakes. Several different types of horizontal pendulums are used to measure tilt amplitudes, possibly except in the Bonchkovsky (1962) case where the type of instruments used is not clear, but they are probably "clinometers" - horizontal pendulums used for earth tide work. The data collected here, both from the literature and our own instruments are sufficiently strong in their consistency to rule out instrumental effects, especially since different types of instruments and different transducer systems are involved.

V. R. Bonchkovsky (1962) reports tilts recorded at 2430 km and 4950 km from the epicenter of the 4 December 1957 Mongolia earthquake of amplitudes 2.0 and 0.9 sec arc respectively and indicates the tilt directions. Since three instruments in a "0" loop configuration were used at each of the two sites, and no discrepancies were observed, the tilts are real. Bonchkovsky also indicates fault length orientation

and displacements. The length and orientation are in general agreement with those derived by Ben-Menahem and Toksöz (1962). Using Bonchkovsky's fault length of 683 km, the tilt stations Garm and Sinderopol are at a minimum distance of 3.6 and 7.3 fault lengths respectively. Depth of the fault was estimated by Ben-Menahem and Toksöz to be 50 km, roughly 1/10 of the fault length. The highest amount of displacement along the fault was about 8 m (Bonchkovsky, 1962) or a few times  $10^{-5}$  of the fault length, somewhat less than the value of  $\frac{4}{3} \times 10^{-4}$  assumed in the numerical calculations of Press (1965). The amount of tilt calculated at a distance of 4 fault lengths (in the case of strike slip) is about  $10^{-8}$  radians, or 2 mscc of arc (see Figure 3). However, the observed value is 2.0 sec of arc, 3 orders of magnitudes higher (and the estimate is conservative).

Since the installation of the tripartite borehole network in Alaska, the recording sensitivity of the tilt signals has been gradually increased. However, the long-period records are still the most sensitive ones to suddenly occurring tilts such as those associated with large distant and local smaller-magnitude earthquakes. Because of the displacement transducer outputs, they may readily be compared to the calibration displacement response of the recordings, which is now routinely obtained twice a day. Calculations of tilt amplitudes made from the long-period records agree (within reading error) with those obtained from the tilt recordings (through the feedback signal at GLM or the high-frequency cut-off filtered PAX demodulator output). For comparison, Figures 15, 17, 19 and 22 show the long-period records, where Figures 14, 16, 18 and 21 show the tilt records of the same Fairbanks area earthquakes.

In the following tables the data on tilt amplitudes and propagation velocity have been assembled, including the data from Bonchkovsky (1962).

TABLE I

LOCAL EARTHQUAKES

DATE	LOCATION	MAG	EPICENTER	DISTANCE	FOCUS	V(TILT) km/sec	TILT
29 Oct 1968	Rampart, Alaska	6.5	125				1.7 sec
21 June 1969	Fairbanks Area	4.6	15				0.3 sec
25 Aug 1969	Fairbanks	4.25	14				0.1 sec
16 April 1970	Fairbanks	3.2	22.5				
9 June 1970	Minto, Alaska	4.2	64				
28 Aug 1970	Fairbanks	3.5	30.2				
23 Sept 1970	Fairbanks	3.3	27.5				
10 Oct 1970	Fairbanks	3.2	29.0				
11 Oct 1970	Fairbanks	3.0	23.5				
26 Oct 1970	Fairbanks	3.7	30.3				

TABLE II  
DISTANT EARTHQUAKES

DATE	AREA	MAG	DIST	V km/sec	TIILT	REF.
4 Dec 1957	Mongolia	7.75	2430 km 4950		2.0 sec arc 0.9 sec arc	Bonchkovsky
5 June 1970	Eastern Siberia	5.5	3200	3.3 2.9	8 m sec	
27 Aug 1970	Near Coast of Mexico	5.7	6740	2.9	20 m sec	

The amplitude of tilts for the Rampart earthquake on October 29, 1968, has been calculated from the amount of trace offset of the horizontal Wood-Anderson seismometers at the U.S.C. & G.S. College Campus station. All others are from the long-period or the combined long-period and tilt records (see Figures 9 through 22).

Epicenters used for the distant earthquakes are those reported on the preliminary epicenter determination cards of the Coast and Geodetic Survey; the Rampart earthquake was reported by Gedney and others (1969) and the Minto epicenter was taken from the routine computer output of Alaskan earthquakes of the seismic laboratory. All Fairbanks shocks have been hand-located using S-P times of a strong-motion instrument, whenever feasible, and the P arrivals at the local stations. Epicenter, depth, and origin are indicated in Figures 4, 5, and 6 for each individual earthquake. The epicenter locations are probably within less than 2 km of the indicated ones, and depth is probably within the same error limit. A possible exception is the earthquake north of PJD. Except for GEO, or later LV (strong motion), all stations are recorded on 16 mm film with second marks imposed on each individual station allowing a time resolution of about 0.02 sec. All stations appear in Figure 2, to show the location with respect to Fairbanks. The area of Figure 2 is located on Figure 1 by the heavy lines around the GLM triangle.

The epicenter locations near Fairbanks are divided into two distinct areas a.) those located southeast of town in the zone of the 1967 magnitude 6.5 earthquake and its aftershocks (Gedney and Berg, 1969) and b.) some 20 km west of there, south to southeast of the airport area.

The Rampart quake had been reported by Gedney and others (1969). However, the fault plane solution indicated on Figure 4 has been obtained by Gedney (personal communication). The Minto earthquake is located on the northern extension of the fault mapped by Péwé and others (1966). The first motion data gave the solution indicated in Figure 4. As a limiting case, the axis may be slightly rotated clockwise, but the rotation is limited by the dilatation at TNN. The strike then appears to coincide exactly with that mapped further south, and the direction of tilt corresponds to that of the strike slip case from Press in Figure 3. The tectonic implication is that the fault continues much further to the north, is active at present and has a strong left lateral component, whereas Péwé and others only show the western side down with respect to the eastern part. It should be noted that the long-period tilt recordings in this case are opposite in direction to those recorded in the Fairbanks area, thus strengthening the argument that the tilts are real and not instrumental effects.

The velocities with which the tilt steps propagate from the focus to the station (for local shocks) and from the epicenter via the great circle to the station for teleseisms are much lower than the shear wave velocity and range from 2.1 km/sec for locals to about 3.3 km/sec for distant earthquakes (Table I and II). Similar velocities have been reported by Wideman and Major for strain steps. In two cases (9 June, 1970, Minto; and 26 Oct 1970, Fairbanks, Figures 12 and 22), the transverse tilt component seems to have a somewhat higher velocity than the radial component. Also, for some distant earthquakes Wideman and Major have noticed two distinct strain steps with two different velocities, similar to the two steps associated with the eastern Siberia earthquake

of 5 June, 1970 (Table II, Figure II). In none of these cases were the instruments off-scale. This, together with the consistency in the propagation velocities as recorded either by strain meters or the tilt meters, strongly indicates that the strain or tilt steps are real.

#### DISCUSSION

**Tilt Amplitudes:** The earlier section on theory indicates that if the static elastic dislocation model is valid to describe the tilt and strain field resulting from an earthquake, the amplitude-distance relation for tilt varies with distance  $R$  as  $R^{-1}$  to  $R^{-6}$ . The exponent depends on the particular type of fault (strike or dip slip) and the orientation of the station with respect to the fault. Figure 7 gives experimental tilt amplitudes versus distance and the number next to each data point are the magnitudes associated with each earthquake (from Table I and II).

Only for the Mongolian earthquake have tilts been recorded at two different distances, and the amplitude diminishes with distance roughly as  $R^{-1}$  (Figure 7, upper right hand, magnitude 7.75). The heavy lines in the Figure represent the amplitude reduction with distance as  $R^{-1}$ . It can be seen that a change in the exponent from -1 to another value will rotate these lines around the data points, but that considerably more overlap in the magnitudes will occur. To see this more clearly, the intersecting distance of the  $R^{-1}$  lines with 1000 msec arc amplitude have been plotted in Figure 8 versus the magnitude. This is only one of many possible choices to check on the consistency of the data. Other levels (such as 100 msec or 19 msec) also could be used, or, one might want to plot the amplitudes (at a fixed distance) versus magnitude. Either way would reveal any inconsistencies in the data. The

amplitude-magnitude-distance relation that emerges from the data presented is of the form:

$$A(\text{in sec arc}) = \frac{10^{M-4.1}}{R \text{ (in km)}}$$

Only in the strike direction of a vertical dip slip fault does theory predict an amplitude reduction of the form  $R^{-1}$ .

However, the recorded tilt amplitudes are simply several orders higher than theory would predict. Assuming a fault length for magnitude 3 to 3.5 earthquakes to be of the order of 1 km (Wyss and Brune, 1968; Wideman and Major, 1967; and Berkhemer, 1962), the GLM station is some 25 to 30 fault lengths from most of the epicenters (and somewhat more from the Minto earthquake). Tilt amplitudes as reported here at 25 to 30 fault lengths only occur in Press's solution at 2 to 4 fault lengths (strike slip of Figure 3).

#### TILT DIRECTIONS

The first motion distributions in Figures 4 to 6 clearly show that the theoretically required dip slip for the  $R^{-1}$  reduction configuration does not occur and that for Fairbanks earthquakes the GLM station is hardly located on or near the strike of a dip slip fault plane.

The rather consistent directions of tilt are indicative of a consistent direction for the tectonic stress and motion in the Fairbanks area which is in agreement with that obtained by Gedney for the Rampart earthquake (personal communication). The stress is best obtained from the solution of the Minto earthquake (9 June, 1970) and the Fairbanks 23 Sept., 1970; and 11 Oct. 1970 earthquakes. In these cases the first motion distribution (Figures 4 and 6) indicates compression from the SSE and NNW, and the tilt directions at least (for Minto and 23 Sept. 1970) corresponds to those obtained from Press (1965) for a surface strike slip fault (the depth of which is half its length and the dislocation is

$\frac{4}{3} \times 10^{-4}$  the length) (Figure 3 and Maruyama, 1964). The other first motion distributions are more complicated and, as shown by Sutton and Berg (1958), small amounts of tilt in the fault and/or auxiliary plane introduce complicated first motion patterns, depending on crustal structure parameters.

#### TECTONIC IMPLICATIONS

The new first motion data presented here and those reported earlier (Gedney and Berg, 1969) imply an almost horizontal compression from the SSE to SE along the northern edge of the Tanana Basin. The first motion data and tilts of the clear solutions (Minto, Figure 4; 23 Sept. and 11 Oct. Figure 6) indicates either left lateral strike slip along almost vertical NNE trending fault or right lateral faulting along the other plane at a depth of nearly 20 km. In the Fairbanks area, these directions are only slightly different from those of approximately located, but questionable surface faults in the Cripple Creek area (Péwé and others, 1966), and the general northeasterly alignment of structural trends in the Birch Creek Schist. The consistently south-easterly tilt at GLM seems to indicate that the area is pushed up and northwest against the mountains in a direction roughly parallel to the eastern section of the Denali fault or perpendicular to the well-defined northwestern edge of the seismic zone, reaching from Cook Inlet along the western part of the Alaskan Range into the Tanana Basin.

The earthquakes nearest to the station HPP also indicate fault activity in a hitherto quiescent area southwest of Fairbanks and at a depth of some 20 km, coinciding with the northern side and the western part of a gravity low. The aftershock zone of the 1967 earthquake and epicenters of the shocks on the right hand side of Figure 6 are associated with the northern edge and the eastern part of this gravity low.

The epicenter north of PJD similarly indicates that the recently mapped thrust fault contact zone (Forbes, personal communication) is an active fault. This fault trends ENE, more or less along the Chatanika River and is also perpendicular to the direction of compression deduced from the Fairbanks earthquakes.

Finally it might be pointed out that the static elastic dislocation model is unable to accommodate the anisotropic propagation found for the 9 June, Minto and 26 Oct. 1970, Fairbanks earthquakes, nor is it able to account for the dual velocities and deformations, and propagation with distinctly different velocities observed by Wideman and Major (1967) for several earthquakes, or the data observed during the present study in form of tilt steps.

#### CONCLUSIONS

In conclusion, the following results have been obtained:

- a.) Real deformation steps have been observed for relatively small earthquakes (down to magnitude 3) located in the lower half of the crust.
- b.) The recorded tilt amplitudes from local as well as more distant earthquakes can roughly be given by a relation of the form:

$$A \text{ (in sec arc)} = \frac{10^{M-4.1}}{R \text{ (in km)}}$$

where A = tilt amplitude

R = distance to epicenter

M = magnitude

and do not verify the tilt amplitudes calculated from static dislocation models.

- c.) Tilt directions in several rather simple strike slip situations are consistent with those predicted by theoretical static elastic dislocation.
- d.) The velocities associated with tilt steps of near earthquakes are lower than shear wave velocities and lower than those reported for strain steps, and sometimes show anisotropic propagation. They range from 2.1 to 2.8 km/sec. This velocity is based on travel time and distance from the focal point to the station. Velocities associated with tilt steps of distant earthquakes are the same (2.9 to 3.3 km/sec) as reported for strain steps over continental paths.
- e.) The deformation propagation in the form of tilts with reduction as  $R^{-1}$  and nearly uniform velocities, lower than the shear wave velocities, suggest a propagation mechanism which is confined to the crust and perhaps to parts of the upper mantle.
- f.) The earthquake tilts and first motions imply a south-southeast to north-northwest compression along the northern edge of the Tanana Basin. The earthquake locations and depths indicate active fault areas south of Fairbanks along a gravity low, along the Chatanika River and on the northern extension of the Minto fault. Some of these faults have not been known to exist and are buried under sediments.

## DEFORMATION AND FAILURE IN AN EARTHQUAKE ZONE

Contribution by Eduard Berg  
and Data Analysis by Niki Bloom

The research reported in this section was partially supported by an AEC contract.

The problem of understanding crustal failure requires relating measurable physical quantities to the stress state of the crustal rock and, if possible, to its time history. This can be achieved relatively easily in the laboratory, but application to earthquake seismology is vastly more complex. Among those parameters are: strain and tilts, resistivity, elastic wave velocities and their ratios, changes in the earth's magnetic field and perhaps heat flow.

### a.) Earthquake Statistics and Stress

Comprehensive laboratory experiments relating to micro-fracturing and their interpretation have been performed by a number of authors, Mogi, Scholz, Brace, and Byerlee to name a few, directly interested in crustal rock. Results show that the Gutenberg-Richter relationship  $\log N = a + b(8-M)$  ( $N$  = number of events of magnitude  $M$  or larger,  $a$  and  $b$  are constants) originally derived from earthquakes, also holds for rock samples subjected to microfracturing in the laboratory. Different "b" values seem to reflect different levels of stress state. (Scholz 1968). On the other hand "b" values for earthquakes are sometimes found to be characteristic for the seismicity of a given area and also vary with depth. Hence, one might argue that regional and depth variation of "b" reflects variation of stress level. The connection between "b" values and relative stress is also indicated by studies of

earthquake foreshock and aftershock series (Berg, 1968). A variation of "b" values for foreshocks of different magnitude main shocks is observed: small "b" implies that high stresses are accumulated in small areas and then small main shocks occur. Similarly, large "b" values (up to 0.6) seem to precede large earthquakes, but indicate a lower overall relative stress.

b.) Deformation Prior to Failure

Final failure is preceded by a rapidly increasing non-elastic deformation, as borne out by many laboratory experiments and their interpretation by microscopic dislocation theory. In an earthquake area such deformation has been measured by strain and tilt meters (see earlier section) or geodetic surveys, and is accompanied by changes in electric resistivity, seismic velocity and the earth's magnetic field. Seismic strain release also shows this rapid exponential increase prior to failure. This exponential increase is expected from dislocation theory. Johnston and Gilman (1959) indicate that the plastic strain rate of a crystal may be written:  $\dot{\epsilon} = b n v$  where  $b$  is the Burgers vector,  $n$  the number of dislocations per unit area and  $v$  the average dislocation velocity, and that the experimental relation between dislocation density and strain is that  $n$  is proportional to strain ( $n = c \cdot \epsilon$ ). On the other hand the dislocation velocity depends on temperature  $T$  and stress  $\tau$  (Johnston and Gilman, 1959 and Gilman, 1965) as  $v = v_0 e^{\frac{-A}{\tau T}}$  for a relatively narrow temperature range, where  $A$  is a constant in first approximation. Combining the two equations results in:  $\dot{\epsilon} = c \epsilon b v_0 e^{\frac{-A}{\tau T}}$  where  $v_0$  is the limiting dislocation velocity usually taken as the shear wave velocity. Integrating with respect to time  $t$  leads to  $\log \epsilon = t c b v_0 e^{\frac{-A}{\tau T}}$  or an exponential

increase in strain with respect to time (under constant temperature and stress). Impurities in the crystal tend to complicate the picture and alter the constants involved, but the basic physical process is conserved. This exponential increase in strain and seismic strain release has been observed in the laboratory under constant stress by Watanabe (1963) (see Figure 26) and Rummel (1969) on rock samples, by Grosskreutz (1962) for the crack (failure) length of a single aluminum crystal (this is a limiting case) for the seismic strain release prior to the Aleutian magnitude 8.2 earthquake 1958 by Berg (May 1966) and for tilt deformation prior to the magnitude 6.5 earthquake of 1952 by Nishimura (1958) and Berg (Dec. 1966) (see Figure 27).

c.) Dilatancy and  $V_p/V_s$  Ratios.

Brace et al. (1966) have examined the dilatancy of Westerly granite (and other rock materials) due to increased porosity while under compression using up to 8 kbars confining pressure. This pressure is approximately equal to those expected in the Fairbanks hypocentral area and for other crustal earthquakes. Consequently, in keeping with the results of Brace et al., it is expected that the increase in rock porosity with increased stress should result in lowering Poisson's ratio, e.g. the  $V_p/V_s$  ratio. Brace (1966) actually reports the lowering of the P-wave velocity in the direction transverse to the applied stress for increasing stress from laboratory experiments by Matsushima. Laboratory data and theoretical considerations (Wachholz, 1966; Schuppe, 1966, and Walsh, 1965) show that Poisson's ratio is a function of porosity and in general decreases with increasing porosity. Brace et al. (1966) have measured maximum departures of the stress volumetric strain curve from the line representing elastic behavior, which is a net volume

increase due to the opening fractures (or the porosity) of the order of 1% (their D values in Table I for granite samples under confining pressures up to 5 kbars). Wachholz's theoretical curves for limestones and sandstones would give a 0.004 decrease in Poisson's ratio for a 1% increase in porosity or a change of about 0.1 in the Vp/Vs ratio (at Vp/Vs = 1.7). This value of 0.1 change is precisely that observed by Semenov (1969) in the Garm region prior to some large earthquakes in the magnitude 5 to 6 range (Russian K from 11 to 13). This short analysis of data available from the literature shows that the observations are consistent with laboratory measurements and theoretical consideration. Analysis was, therefore, attempted of Vp/Vs ratios of earthquakes in the micro-earthquake net around Fairbanks in addition to the variation of the "b" values. The method used to obtain Vp/Vs has been described by Gedney and Berg (1969) for a homogeneous crust.

#### d.) Results of Micro-Earthquake Analysis in the Fairbanks Area.

The only example of decreasing "b" value over a short time interval is that reported earlier (Berg, 1970) for a magnitude 4.9 earthquake that occurred near Fairbanks. Niki Bloom, a graduate student, analyzed the micro-earthquakes for the month of March, 1970, when some 400 were recorded. The magnitude range spans approximately -1.0 to 3.0. The minimum number recorded was 5 shocks per day on three days and 20 or more have been recorded on three days. This data has been analyzed for variation of "b" with time and variation of the Vp/Vs ratio. Not all earthquakes have been detected simultaneously at all stations. Micro-earthquakes that occurred during October, 1970, are now being analyzed, because other information on crustal tilt and precise location of several earthquakes with magnitudes larger than 3 is available (see section on tilts associated with earthquakes).

Results concerning the time variation of the "b" slope are not very conclusive. Sample size to determine "b" usually was about 60 earthquakes. It is noted that the log N versus M curve is often represented by two branches rather than one, a fact that Mogi (1962) attributes to the structural length dimensions in the focal area. However, work on fracturing of glass (under thermal shock) shows that stress redistribution during crack propagation is significant (Chi-Yu King, 1965), and the "stress front" in front of a propagating crack (fault) superimposed on the tectonic stress might be responsible for crack division processes that lead to the break in the log N versus M plots as a function of stress.

Results of determination of Vp/Vs are presented in Figure 28. Dots indicate that P and S wave arrivals at three stations have been used to determine the value, whereas circled dots have been determined from data of four stations, using a single layered earth crust model. The large scatter in the data obtained from three stations only suggest that more precise values might be obtained with more stations and that the orientation of the wave path with respect to the stress axis should perhaps be considered. Therefore, two new short-period vertical seismometers have been added to the micro-earthquake network. These stations are Hepp (HPP) and Birch Hill (BRH) (Figure 2).

**PUBLICATIONS AND REPORTS, ACKNOWLEDGING  
AFOSR SUPPORT FROM THIS CONTRACT**

**Berg, Eduard, and Ronald Rasmussen:** Technical Report, The Effect of Barometric Pressure Variation on the "U.S.O." Long-Period Seismometer, Geophysical Institute, University of Alaska, Feb., 1970.

**Berg, Eduard and Hans Pulpan:** Tilts Associated With Small and Medium Size Earthquakes. Paper presented by E. Berg at the Geophysical Institute, University of Tokyo, Tokyo, Japan, on December 19, 1970; Sent to: Journal of Physics of the Earth, Jan., 1971.

**Berg, Eduard:** Seismology and Tectonics of Alaska, Paper presented: Inaugural Symposium, Geophysical Institute, University of Alaska, June 30, 1970, referenced in: Annual Report 1969-70, Geophysical Institute, University of Alaska, p 101.

**PUBLICATIONS, ACKNOWLEDGING EARLIER AFOSR SUPPORT**

**Davies, John N.:** Crustal Morphology of Central Alaska, M.S. Thesis, University of Alaska, 57 pages including 24 Figures, May, 1970, AFOSR Contract F-44620-68-C-0066.

**Kienle, Jürgen:** Gravity Traverses in the Valley of Ten Thousand Smokes, Katmai National Monument, Alaska, Journal of Geophysical Research, Vol. 75, No. 32, pp. 6641-6649, Nov. 10, 1970, AFOSR Grant 701-66.

**Gedney, Larry:** Tectonic Stresses in Southern Alaska in Relation to Regional Seismicity and the New Global Tectonics, Bulletin of the Seismological Society of America, Vol. 60, No. 6, pp. 1789- 1802, Dec. 1970, AFOSR Contract F-44620-68-C-0066.

## REFERENCES

Ben-Menahem, Ari, and Nafi M. Toksöz: Source-Mechanism from Spectra of Long-Period Seismic Surface Waves, *Journal of Geophysical Research*, Volume 67, No. 5, pp. 1943-1955, May 1962.

Ben-Menahem, Ari, Sarva Jit Singh and Faiza Solomon: Static Deformation of a Spherical Earth Model by Internal Dislocations, *Bulletin of the Seismological Society of America*, Volume 59, No. 2, pp. 813-853, April, 1969.

Ben-Menahem, Ari, Sarva Jit Singh, and Faiza Solomon: Deformation of a Homogeneous Earth Model by Finite Dislocation, *Review of Geophysics and Space Physics*, Vol. 8, No. 3, pp. 541-632, August, 1970.

Berckhemer, H.: Die Ausdehnung der Bruchfläche im Erdbebenherd und ihr Einfluss auf das seismische Wellenspektrum. *Gerlands Beiträge zur Geophysik* Band 71, No. 1, pp. 5-26, 1962.

Berg, Eduard: Fundamental and Applied Research in Seismology in Alaska, *Geophysical Institute, University of Alaska, Research Report UAG R-179*, May, 1966.

Berg, Eduard: Triggering of the Alaskan Earthquake of March 28, 1964, and Major Aftershocks by Low Ocean Tide Loads, *Nature*, Vol. 210, No. 5039, pp. 893-896, 1966.

Berg, Eduard: Deformation Release and Failure in an Earthquake Zone Abstract, *Transactions, American Geophysical Union*, Vol. 47, No. 4, p. 626, December, 1966.

Berg, Eduard: Relation Between Earthquake Foreshocks, Stress, and Mainshocks, *Nature*, Vol. 219, No. 5159, pp. 1141-1143, Sept. 14, 1968.

Berg, Eduard: Tectonic Movement, Deformation Release and Crustal Structure Studies in Alaska, *Final Report AFOSR Contract F-44620-68-C-0066*, January 1970.

Bonchkovsky, V. R.: Deformations of the Earth's Surface Accompanying Certain Disastrous Distant Earthquakes, (*Bulletin "Izvestiya Geophys. Ser."*) pp. 190-193, 1962. (english ed.), pp. 132-134.

Brace, W. R., B. W. Paulding, Jr., and C. Scholz: Dilatancy in the Fracture of Crystalline Rocks, *Journal of Geophysical Research*, Vol. 71, No. 16, pp. 3939-3953, August, 1966.

Carder, D. S.: Seismic Investigations in the Boulder Dam Area, 1940-1944, and the Influence of Reservoir Loading on Local Earthquake Activity, *Bulletin of the Seismological Society of America*, Vol 35, pp. 175-192, 1945.

**Chinnery, M. A.: The Deformation of the Ground Around Surface Faults,**  
**Bulletin of the Seismological Society of America, Vol. 51, No. 3,**  
**pp. 355-372, July, 1961.**

**Davies, John N.: Crustal Morphology of Central Alaska, a Thesis for**  
**M. S., University of Alaska, Geophysical Institute, May, 1970.**

**Gedney, Larry, and Eduard Berg: The Fairbanks Earthquake of June 21,**  
**1967; Aftershock Distribution, Focal Mechanisms, and Crustal**  
**Parameters, Bulletin of the Seismological Society of America,**  
**Vol. 59, No. 1, pp. 73-100, February, 1969.**

**Gedney, Larry, Eduard Berg, Hans Pulpan, John Davies, and William Fetham:**  
**A Field Report on the Rampart, Alaska Earthquake of October 29, 1968,**  
**Bulletin of the Seismological Society of America, Vol. 59, No. 3,**  
**pp. 1421-1423, June 1969.**

**Gilman, J. J.: Dislocation Mobility in Crystals, Journal of Applied**  
**Physics, Vol. 36, No. 10, pp 3195-3206, October , 1965.**

**Gough, D. I. and W. I. Gough: Load-triggered Seismic Activity at**  
**Lake Kariba, Transactions, American Geophysical Union, Vol. 50,**  
**No. 4, pp. 236, April, 1969.**

**Gough, D. I. and W. I. Gough: Stress and Deflection in the Lithosphere**  
**near Lake Kariba (Paper I), Department of Physics, University of**  
**Alberta, Edmonton Alberta, Canada, 21 pages and 8 figures, Pre-**  
**print, March, 1970.**

**Grosskreutz, J. C.: Fatigue Crack Propagation in Aluminum Single**  
**Crystals, Journal of Applied Physics, Vol. 33, No. 5, pp. 1787-**  
**1792, May, 1962.**

**Hagiwara, Takahiro: Observations in the Changes in the Inclination of**  
**the Earth's Surface at Mt. Tukuba, Bulletin of the Earthquake**  
**Research Institute, Vol. XVI, Part 2, pp. 366-371, 1938.**

**Hagiwara, Takahiro: Observations of Tilting of the Ground due to**  
**Matsushiro Swarm Earthquakes, Transactions, American Geophysical**  
**Union, Vol. 50, No. 5, pp. 391, May, 1969.**

**Healy, J. H., W. W. Rubey, D. T. Griggs, and C. B. Raleigh: The**  
**Denver Earthquakes, Disposal of waste fluids by injection into**  
**a deep well has triggered earthquakes near Denver, Colorado,**  
**Science, Vol. 161, No. 3848, pp. 1301-1310, September 27, 1968.**

**Johnston, W. G. and J. J. Gilman: Dislocation Velocities, Dislocation**  
**Densities, and Plastic Flow in Lithium Fluoride Crystals, Journal**  
**of Applied Physics, Vol. 30, No. 2, pp. 129-144, February, 1959.**

Karmaleeva, R. M.: An Attempt to Forecast the Time of Near Earthquakes, Bulletin (Izvestiya) (Geophys. Ser.), pp. 467-474, 1960. (english edition) pp. 308-312.

Karmaleeva, R. M.: On Certain Coincidences Between Anomalous Tilt and the Occurrence of Earthquakes, Bulletin (Izvestiya) (Geophys. Ser.) No. 11, pp. 1557-1561, November, 1962, (english ed.), pp. 970-972 1962.

King, Chi-Yu: Internal Fracture of Glass by Thermal Shock, Report Number 411, Materials Science Center, Cornell University, Ithaca, New York, September, 1965.

Maruyama, Takuo: Statical Elastic Dislocations in an Infinite and Semi-Infinite Medium, Bulletin of the Earthquake Research Institute, Vol. 42, pp. 289-368, 1964.

McGinnis, L. D.: Earthquakes and Crustal Movement as related to Waterload in the Mississippi Valley Region, Illinois State Geological Survey, Urbana Circular 344, 1963.

Nishimura, Eiichi: Some Problems of Tilting Motion of the Ground, Deuxième colloque International de la Commission du CSAGI pour l'étude des marées terrestres (Munich 21-26 Juillet 1958) Communications de l'Observatoire Royal de Belgique, No. 142, Série Géophysique, No. 47, pp. 100-110, 1958.

Ozawa, Izuo: On the Combined Observations of the Crustal Deformation at some Observatories in the short intervals, in Geophysical Papers dedicated to Professor Kenzo Sassa, pp. 427-433, 1963.

Péwé, Troy L., Clyde Wahrhaftig and Florence Weber: Geological Map of the Fairbanks Quadrangle, Alaska. Miscellaneous Geological Investigations, Map I - 455, The U.S. Geological Survey, Washington, D. C., 1966.

Press, Frank: Displacements, Strains, and Tilts at Teleseismic Distances, Journal Geophysical Research, Vol. 70, pp. 2395-4212, May 15, 1965.

Rothé, J. P.: Fill a lake, start an Earthquake, New Scientist, pp. 75-78, July 11, 1968.

Rummel, F.: Studies of time-dependent deformation of some granite and eclogite rock samples under uni-axial, constant compressive stress and temperatures up to 400°C, Zeitschrift für Geophysik, Band 35, pp. 17-42, 1969.

Sassa, Kenzo, and Eiichi Nishimura: On Phenomena Forerunning Earthquakes, Transactions, American Geophysical Union, Vol. 32, No. 1, pp. 1-6, 1951.

Scholz, C. H.: The Frequency-Magnitude Relation of Microfracturing in Rock and its Relation to Earthquakes, Bulletin of the Seismological Society of America, Vol. 58, No. 1, pp. 399-415, February, 1968.

Schuppe, F.: Ein Beitrag zur Deutung des Elastischen Verhaltens von Gesteinen beim Durchgang von Körperschall, Gerlands Beiträge zur Geophysik, Vol. 75, pp. 319-323, 1966.

Semenov, A. M.: Variations in the Travel-Time of Transverse and Longitudinal Waves before Violent Earthquakes. (Izvestiya)(engl. ed.) Earth Physics, No. 4, pp. 245-248, (engl. transl.), 1969.

Singh, S. J. and Ari Ben-Menahem: Displacement and Strain Fields Due to Faulting in a Sphere, Physics of the Earth and Planetary Interiors, 2, pp. 77-87, 1969.

Sutton, George H. and Eduard Berg: Direction of Faulting from First-Motion Studies. Bulletin of the Seismological Society of America, Vol. 48, pp. 117-128, April, 1958.

Verbaandert, J. et P. Melchior: La Station de Pendules Horizontaux de Sclaigneaux (Province de Namur), Communications de l'Observatoire Royal de Belgique No. 170, Série de Géophysique No. 54, Bulletin de l'Academie Royale de Belgique (Classe des Sciences), pp. 1084, Séance du samedi, 6 fevrier, 1960.

Wachholz, H.: Poisson's Constant with Dry Sediments and with Packings of Spheres, Geophysical Prospecting, Volume XIV, pp. 204-215, 1966.

Walsh, J. B.: The Effect of Cracks in Rocks on Poisson's Ratio, Journal of Geophysical Research, Vol. 70, No. 20, pp. 5249-5257, October, 1965.

Watanabe, H. 1963, given by Press and Brace: Earthquake Prediction Science, Vol. 52, No. 3729, pp. 1579, June, 1966.

Wideman, C. J., and M. W. Major: Strain steps associated with Earthquakes, Bulletin of the Seismological Society of America, Vol. 57 No. 6, pp. 1429-1444, December, 1967.

Wyss, Max and James N. Brune: Seismic Moment, Stress, and Source Dimensions for Earthquakes in the California-Nevada Region, Journal of Geophysical Research, Vol. 73, No. 14, pp. 4681-4695, July, 1968.

## LIST OF FIGURES

Fig. 1 Geophysical Institute, University of Alaska seismic telemetry system. Triangles-borehole tilt and long-period stations. Large dots-1 sec vertical short-period seismometers. Small dots-U.S.C.G.S. Tsunami Warning Network. The area outlined around the GLM triangle is rendered in detail in Figure 2.

Fig. 2 Fairbanks area seismic telemetry stations and U.S.C.G.S. stations.

Fig. 3 Vector tilt fields, based on Press's (1965) calculation for vertical surface fault, depth equal to half its length, dislocation equal to  $\frac{4}{3} \times 10^{-4}$  of the length. Division on  $x_1$  and  $x_2$  axis equals fault length.

Fig. 4 Upper: Rampart earthquake parameters. Fault motion after Gedney (personal communication). Tilts based on offset of Wood-Anderson horizontal seismometers (U.S.C.G.S. College station).  
Lower: Minto earthquake. Tilt and first motion.

Fig. 5 Chatanika Valley earthquake, first motion and tilt. See also Figure 9 for tilts. The north component is not well defined.

Fig. 6 Fairbanks area earthquakes associated with tilts. Each station given in the local network has been used to determine origin time and focal point. For individual tilt records see later Figures. For fault plane and stress direction determination refer to text.

Fig. 7 Tilt amplitude versus distance. Numbers refer to magnitude of each quake. Heavy lines represent amplitude reduction with distance R as  $R^{-1}$ . For data refer to Tables I and II.

Fig. 8 Distance at which a given magnitude earthquake will generate a 1000 msec arc tilt, using the  $R^{-1}$  amplitude reduction. (Data points are obtained by the distance at which the  $R^{-1}$  reduction heavy line intersects the 1000 msec arc level in Figure 7.).

Fig. 9 Tilts associated with the June 21, 1969, and August 25, 1969, earthquakes in the Chatanika Valley and Fairbanks. Note that only hourly readings have been made during the early recordings at low sensitivity values.

Fig.10 GLM, N-S, long-period record (E-W not available), 16 April, 1970; time marks are minute intervals. Compare the tilt (third trace from top) to the calibration displacement (second trace from bottom).

Fig.11 PAX, 5 June, 1970; note dual tilt step on north-south component and compare to calibration displacement, bottom trace.

Fig.12 GLM, LP, 9 June, 1970, records: from top to bottom: Vertical (unfiltered transducer output) N-S and E-W (filtered).

Fig.13 GLM, 27 August, 1970, LP horizontal records.

Fig.14 GLM, 28 August, 1970, tilt records, compare with Figure 15 for the same quake.

Fig.15 GLM, 28 August, 1970, LP horizontal records, compare tilts with Figure 14.

Fig.16 GLM, 23 September, 1970, tilts, compare with Figure 17.

Fig.17 GLM, 23 September, 1970, LP horizontal records, compare with Figure 16.

Fig.18 GLM, 10 October, 1970, tilts, compare with Figure 19.

Fig. 19 GLM, 10 October, 1970, LP horizontal records, compare with Figure 18.

Fig. 20 GLM, 11 October 1970, LP horizontal records.

Fig. 21 GLM, 26 October, 1970, tilt records, compare with Figure 22.

Fig. 22 GLM, 26 October, 1970, LP horizontal records, compare with Figure 21.

Fig. 23 Tilt on the X-component of GLM, PAX, and MCK and Barometric Pressure at the Fairbanks International Airport.

Fig. 24 PAX tilts from 3 April 1970 to 16 April just prior to the Yakataga earthquake.

Fig. 25 Vector diagram of GLM tilts. Points indicate 6-hourly readings. Note tilt toward the Yakataga area for 3 days, prior to the magnitude 6.8 quake and "S" loop on April 15. Distance to the epicenter is around 650 km.

Fig. 26 Laboratory results for strain and strain release by microfractures in granite, for constant stress and temperature, showing pre-monitory, exponential increase prior to failure. (After Watanabe 1963).

Fig. 27 Tilts prior to the magnitude 6.5 Daishoji-Oki earthquake, 1952.  
a.) original data from Nishimura, 1958.  
b.) tilts towards the epicenter (secular tilts removed from a.)

Fig. 28  $V_p/V_s$  in the Fairbanks area, March 1970, dots based on P and S wave arrivals at 3 stations, circled dots on P and S wave arrivals at 4 stations.



Fig. 1 Geophysical Institute, University of Alaska seismic telemetry system. Triangles-borehole tilt and long-period stations. Large dots-1 sec vertical short-period seismometers. Small dots-U.S.C.G.S. Tsunami Warning Network. The area outlined around the GLM triangle is rendered in detail in Figure 2.

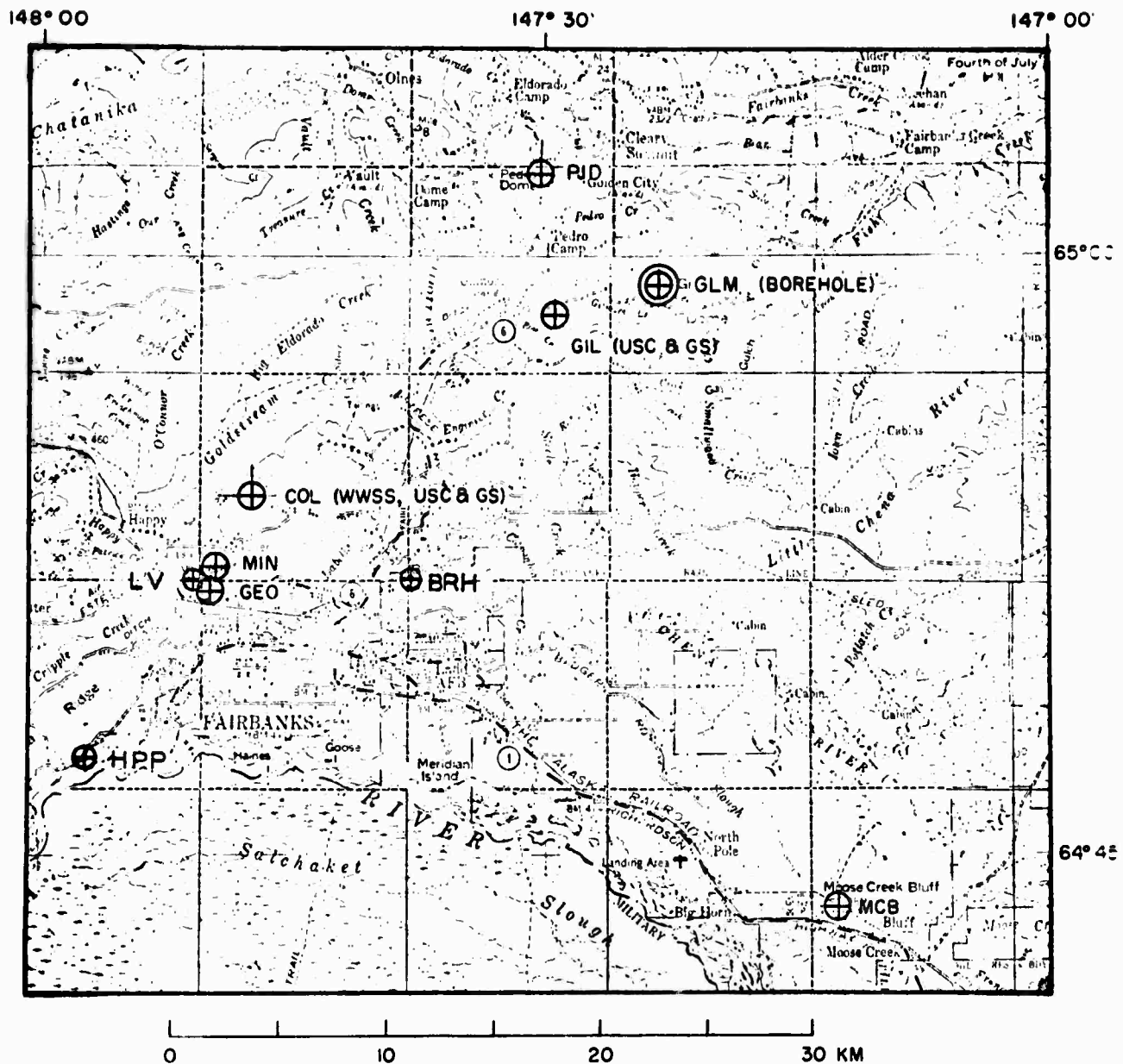


Fig. 2 Fairbanks area seismic telemetry stations and U.S.C.G.S. stations.

42

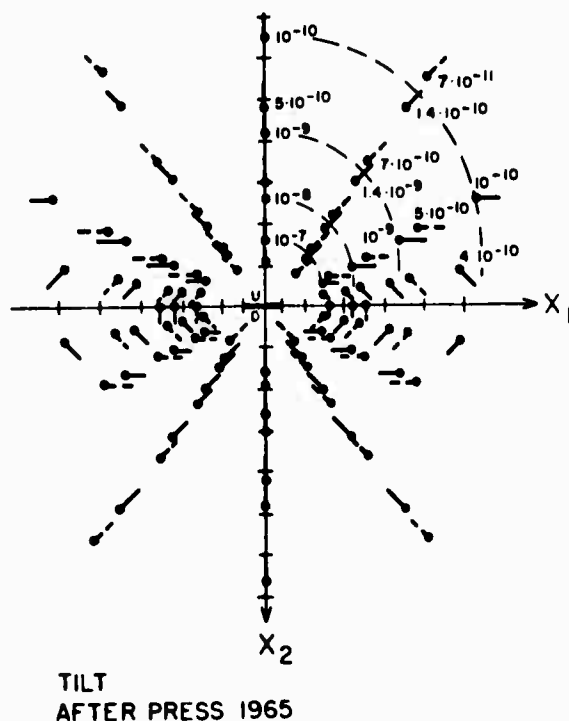
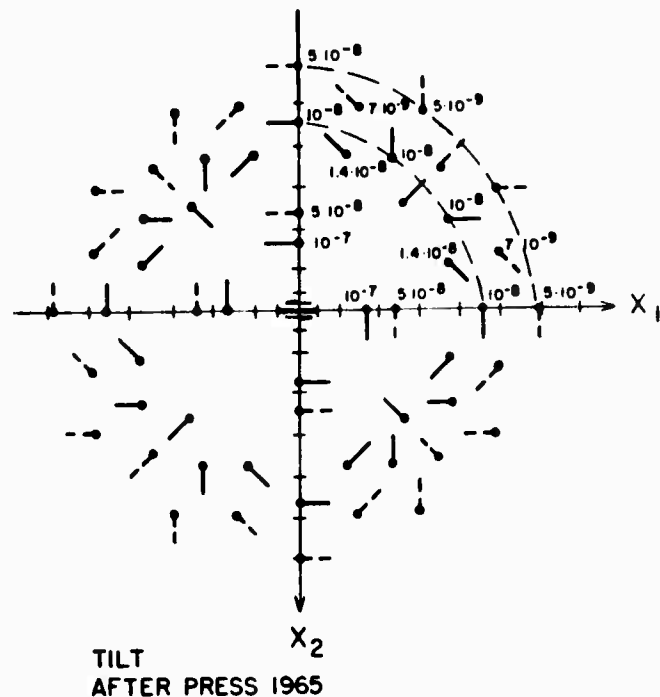


Fig. 3 Vector tilt fields, based on Press's (1965) calculation for vertical surface fault, depth equal to half its length, dislocation equal to  $4 \times 10^{-4}$  of the length. Division on  $x_1$  and  $x_2$  axis equals fault length.

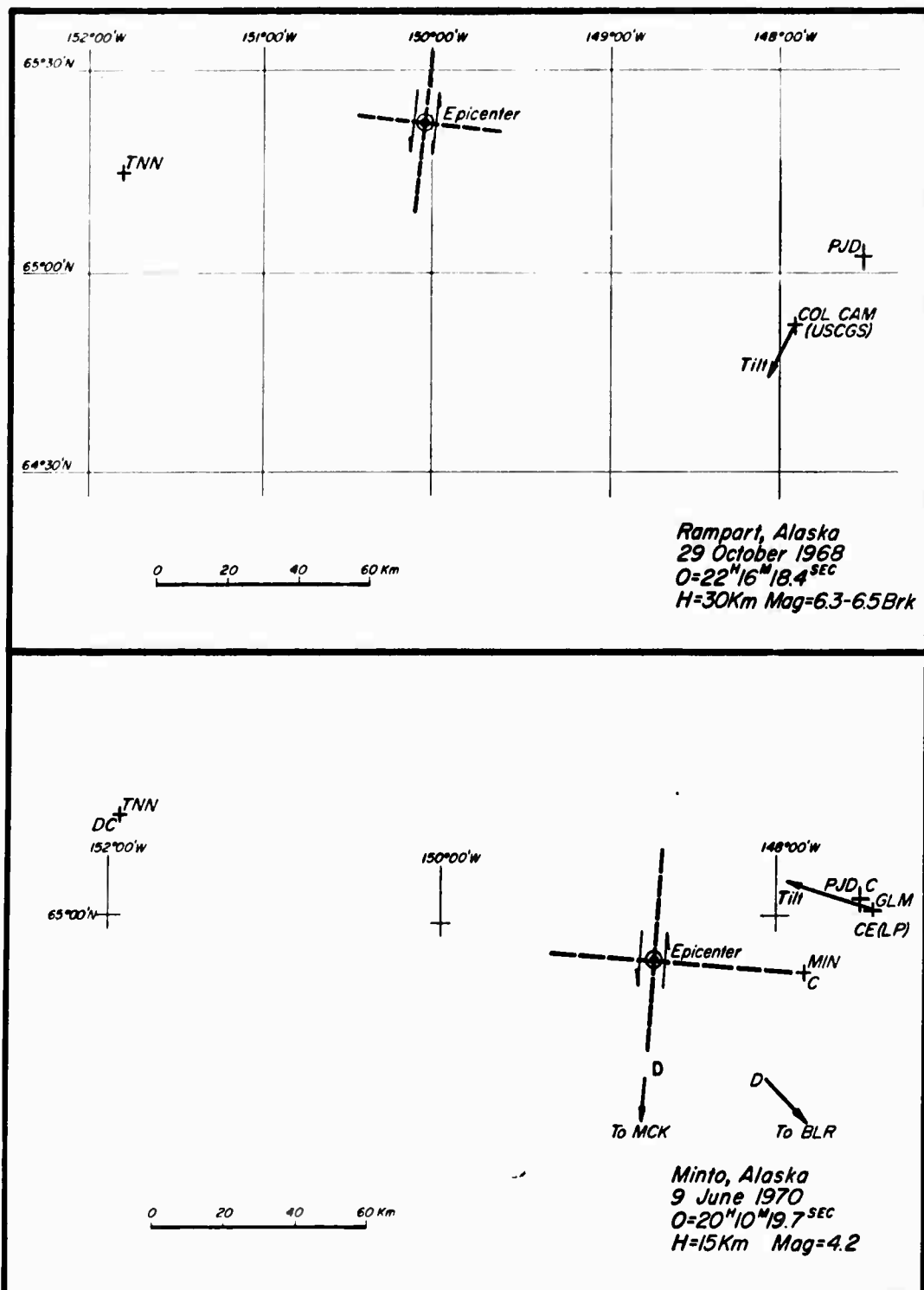
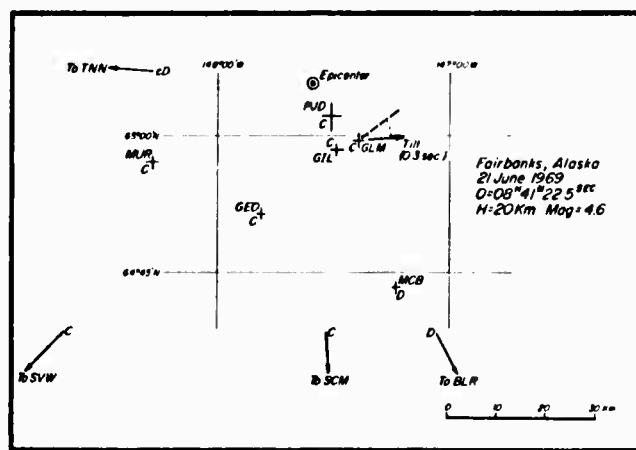


Fig. 4      Upper: Rampart earthquake parameters. Fault motion after Gedney (personal communication). Tilts based on offset of Wood-Anderson horizontal seismometers (U.S.C.G.S. College station).

Lower: Minto earthquake. Tilt and first motion.

44

1000



**Fig. 5** Chatanika Valley earthquake, first motion and tilt. See also Figure 9 for tilts. The north component is not well defined.

45

FIGURE 5

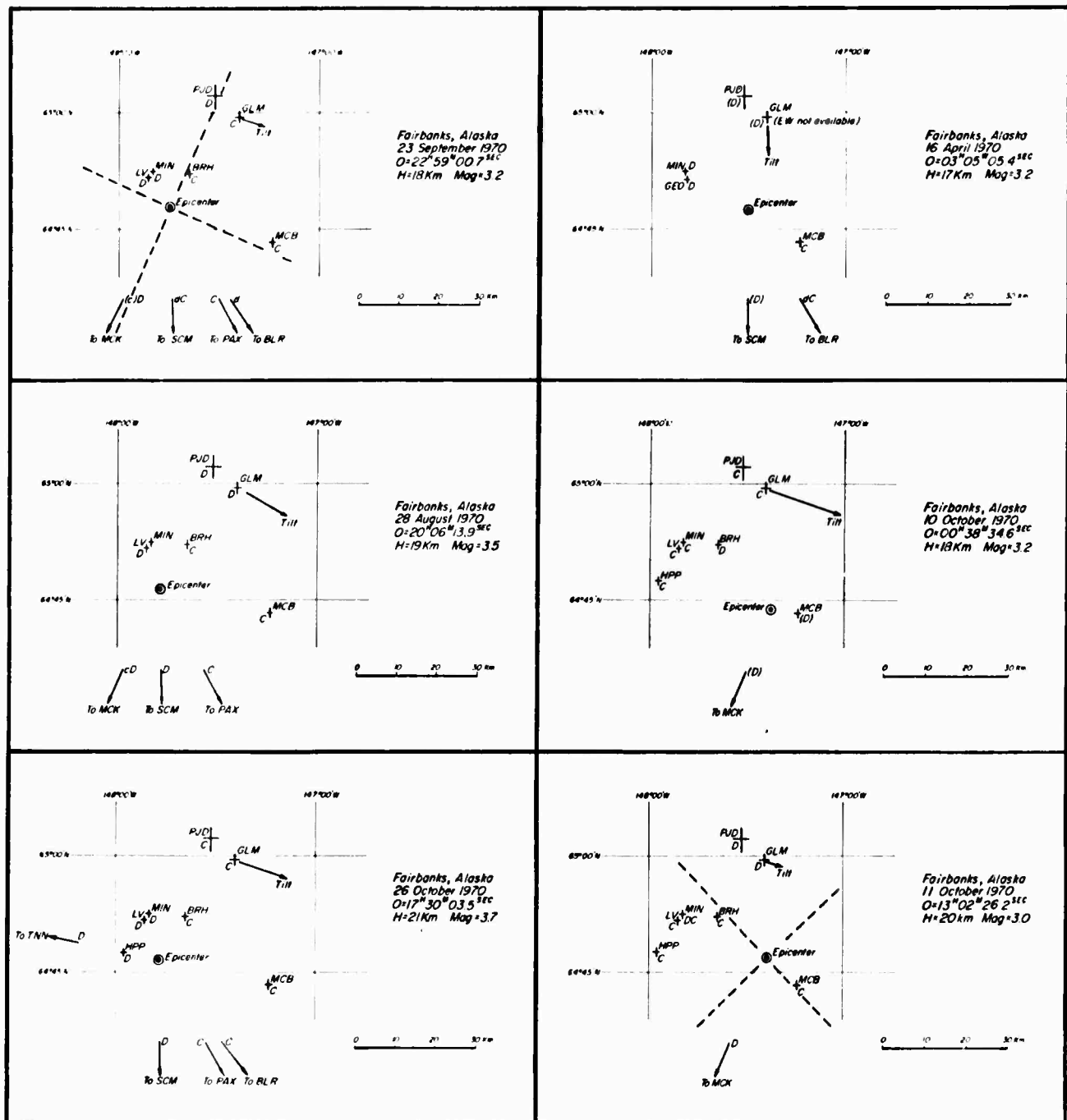


Fig. 6 Fairbanks area earthquakes associated with tilts. Each station given in the local network has been used to determine origin time and focal point. For individual tilt records see later Figures. For fault plane and stress direction determination refer to text.

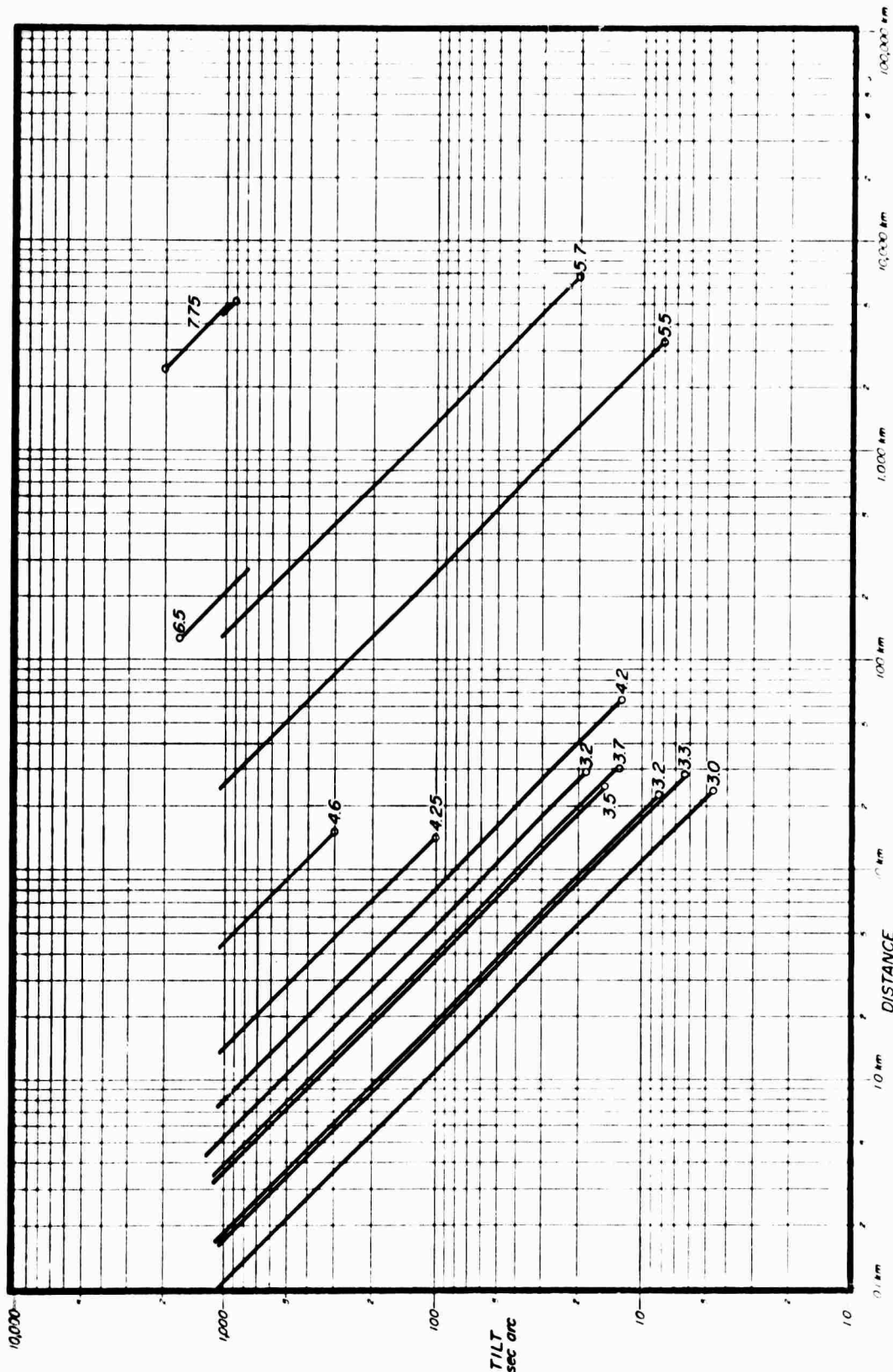


Fig. 7 Tilt amplitude versus distance. Numbers refer to magnitude of each quake. Heavy lines represent amplitude reduction with distance  $R$  as  $R^{-1}$ . For data refer to Tables I and II.

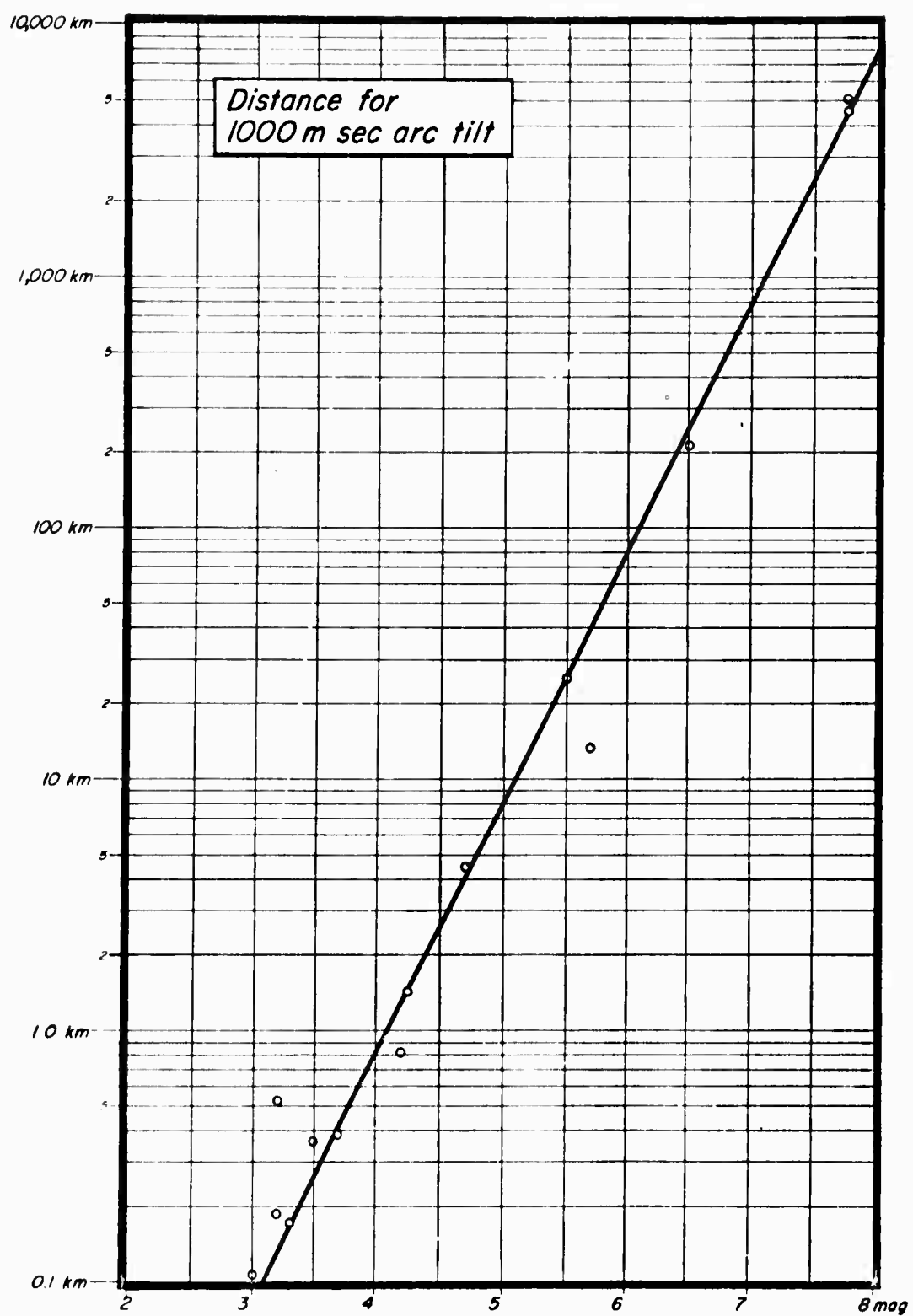
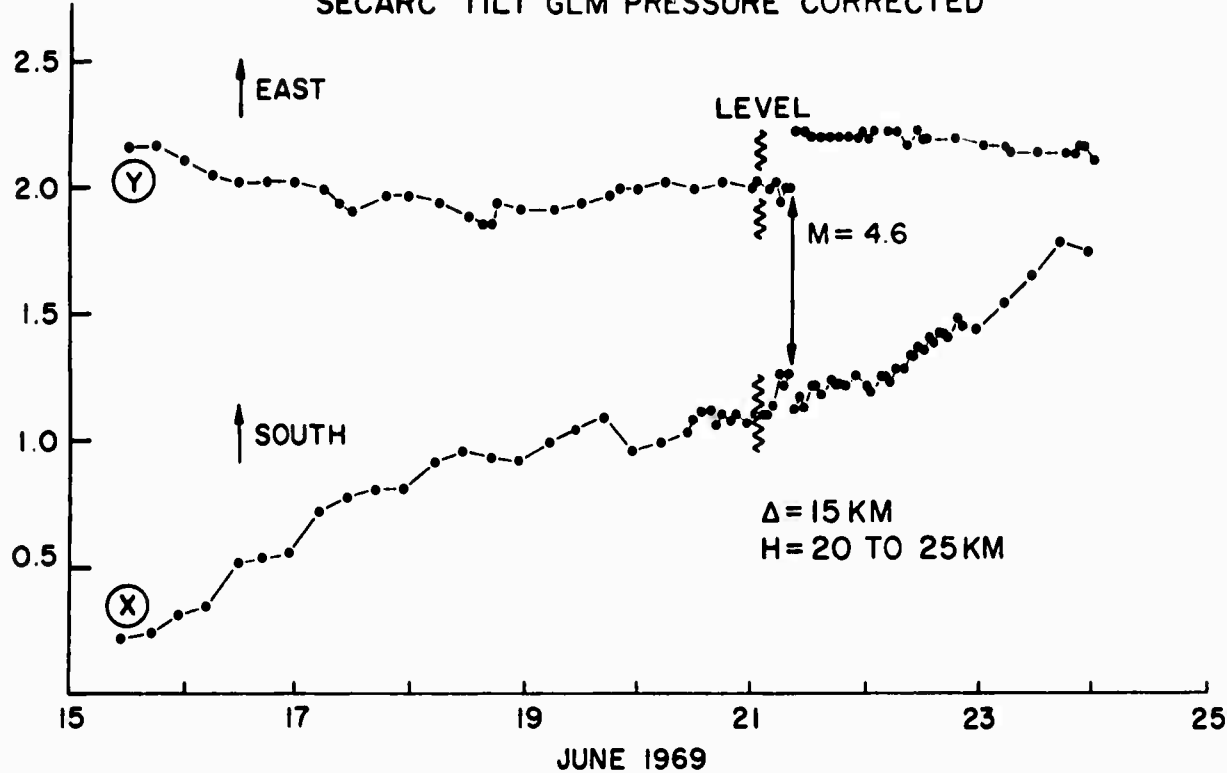


Fig. 8 Distance at which a given magnitude earthquake will generate a 1000 msec arc tilt, using the  $R^{-1}$  amplitude reduction. (Data points are obtained by the distance at which the  $R^{-1}$  reduction heavy line intersects the 1000 msec arc level in Figure 7.).

48

FIGURE 8

SECARC TILT GLM PRESSURE CORRECTED



SECARC TILT GLM PRESSURE CORRECTED

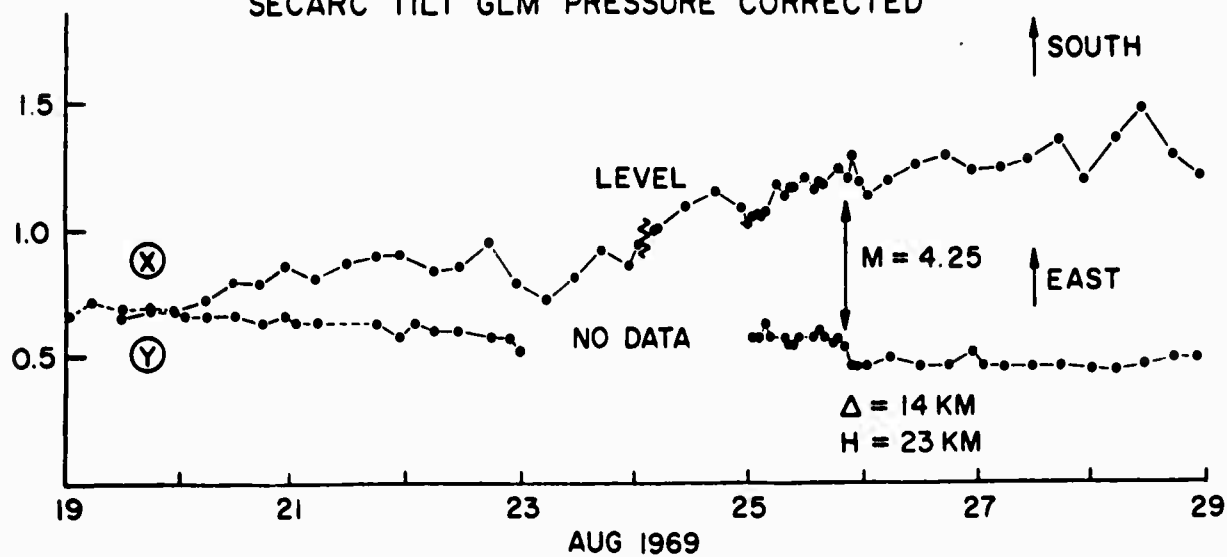


Fig. 9 Tilts associated with the June 21, 1969, and August 25, 1969, earthquakes in the Chatanika Valley and Fairbanks. Note that only hourly readings have been made during the early recordings at low sensitivity values.

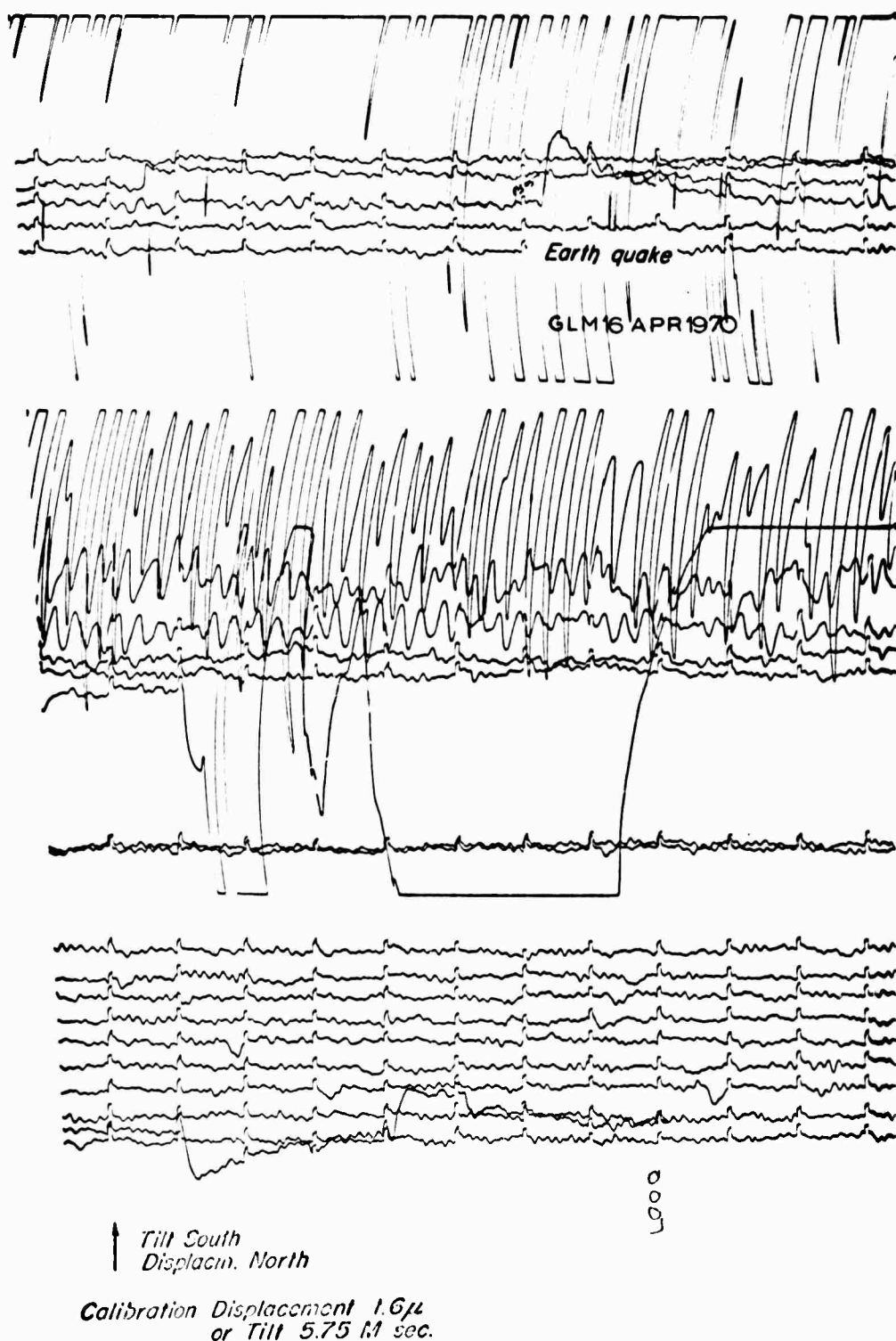


Fig. 10 GLM, N-S, long-period record (E-W not available), 16 April, 1970; time marks are at minute intervals. Compare the tilt (third trace from top) to the calibration displacement (second trace from bottom).

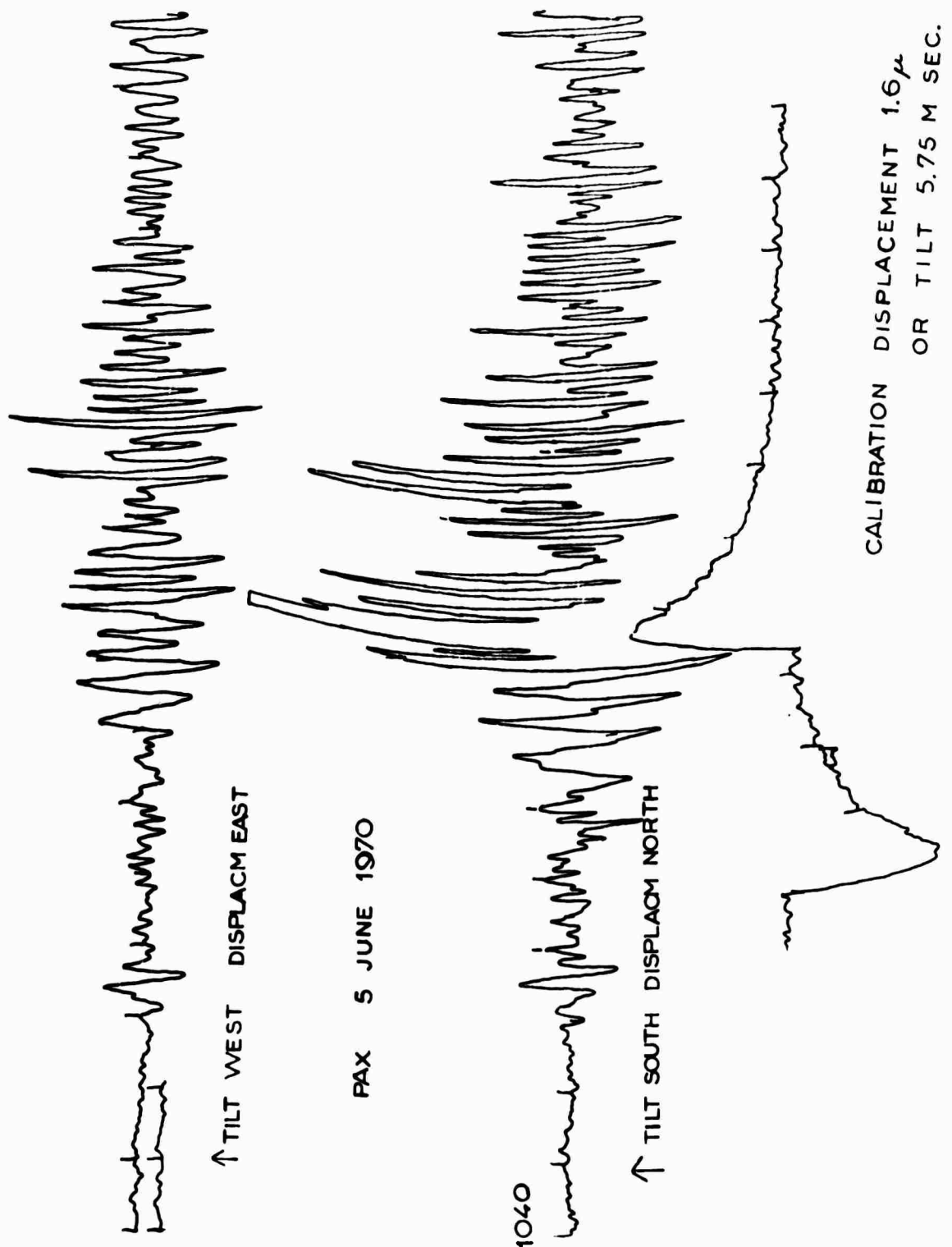
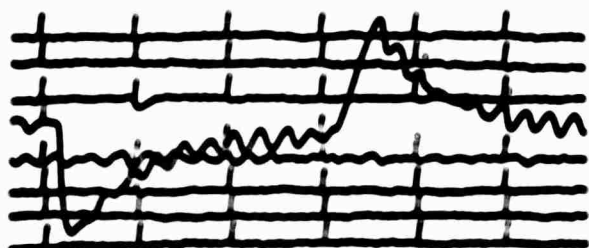
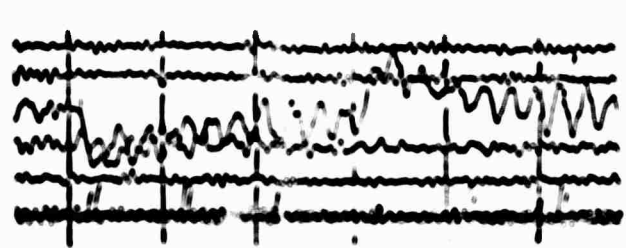
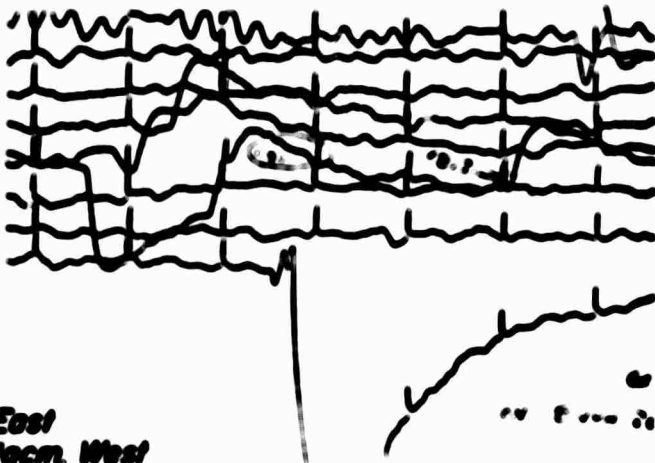
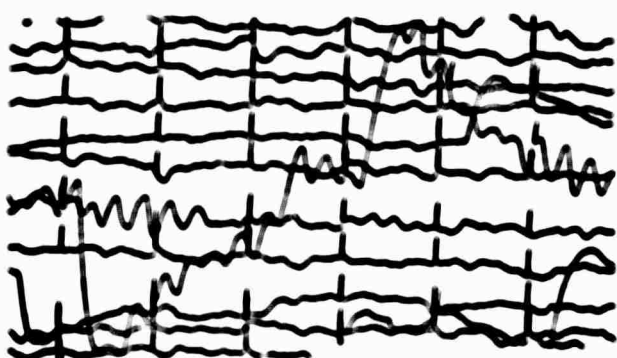


Fig. 11 PAX, 5 June, 1970; note dual tilt step on north-south component and compare to calibration displacement, bottom trace.



↑ TII South  
Displacem. Norm



↑ TII East  
Displacem. West

Calibration Displacement  $1.6 \mu$   
or TII 3.75 M sec.

Earthquake

GLM 9 June 1970 Mag. 4.2

Fig. 12 GLM, I.P., 9 June, 1970, records: from top to bottom: Vertical (unfiltered transducer output) N-S and E-W (filtered).

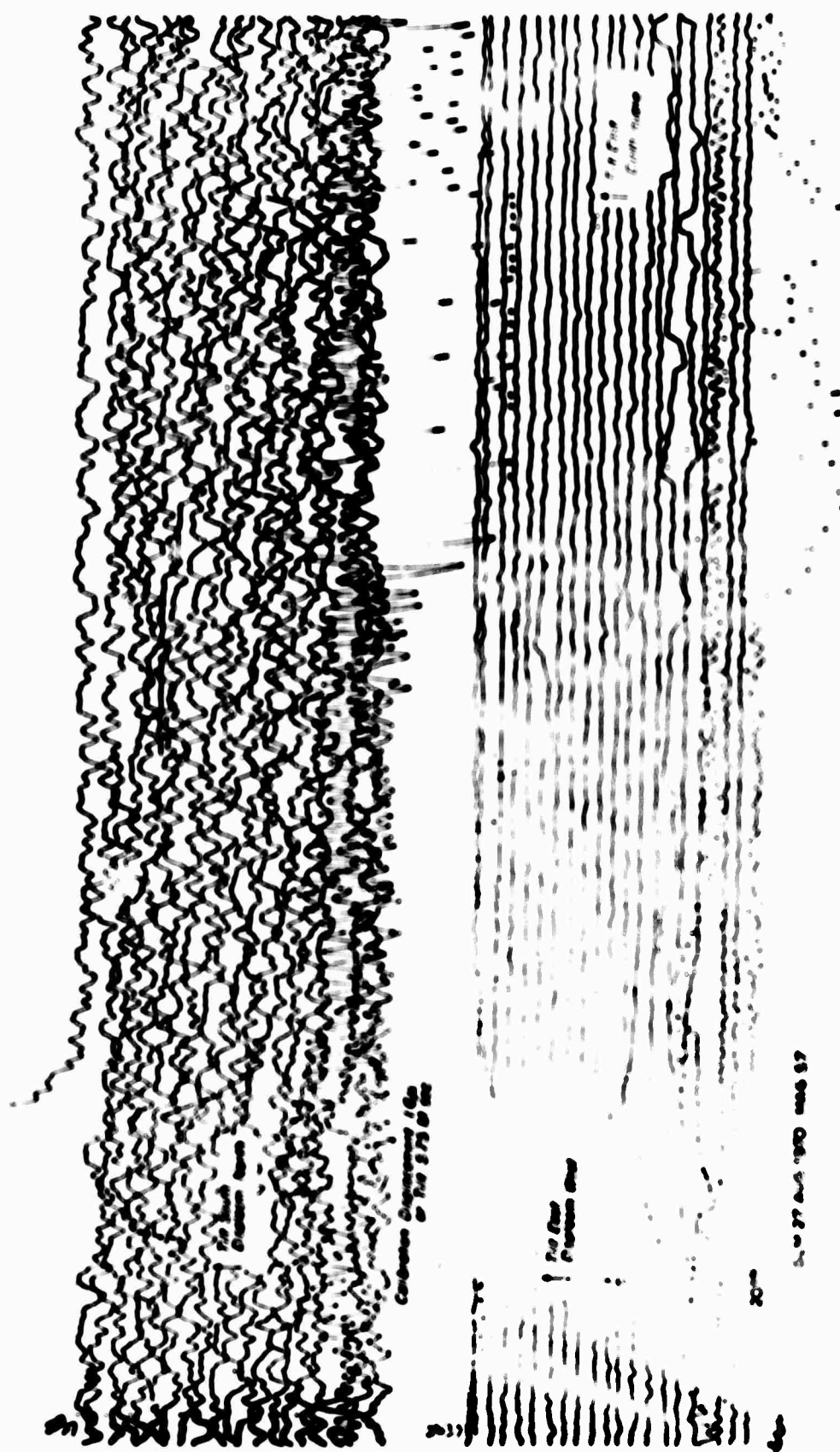


FIG. 13 CLN. 27 August, 1970. LP horizontal records.

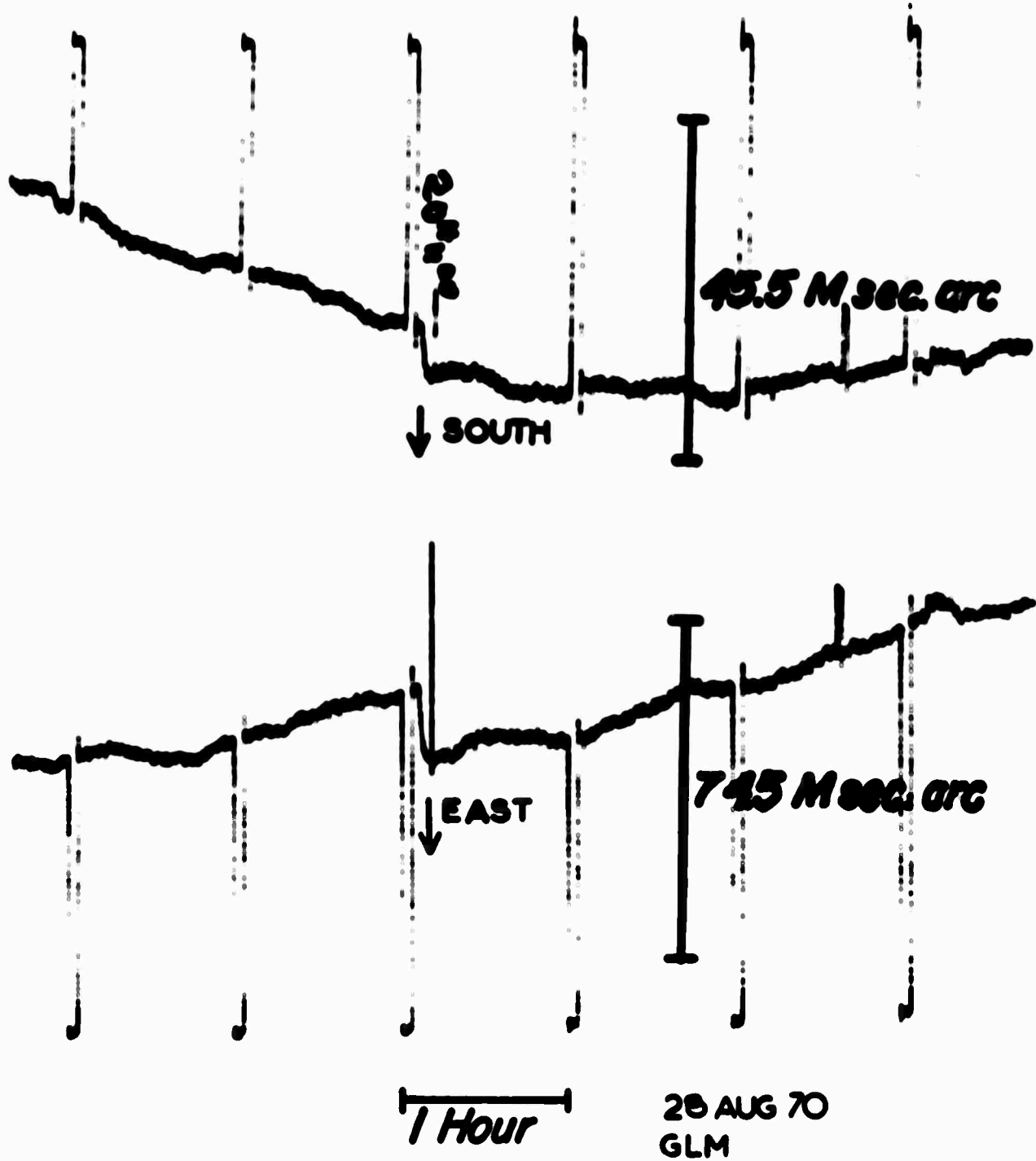
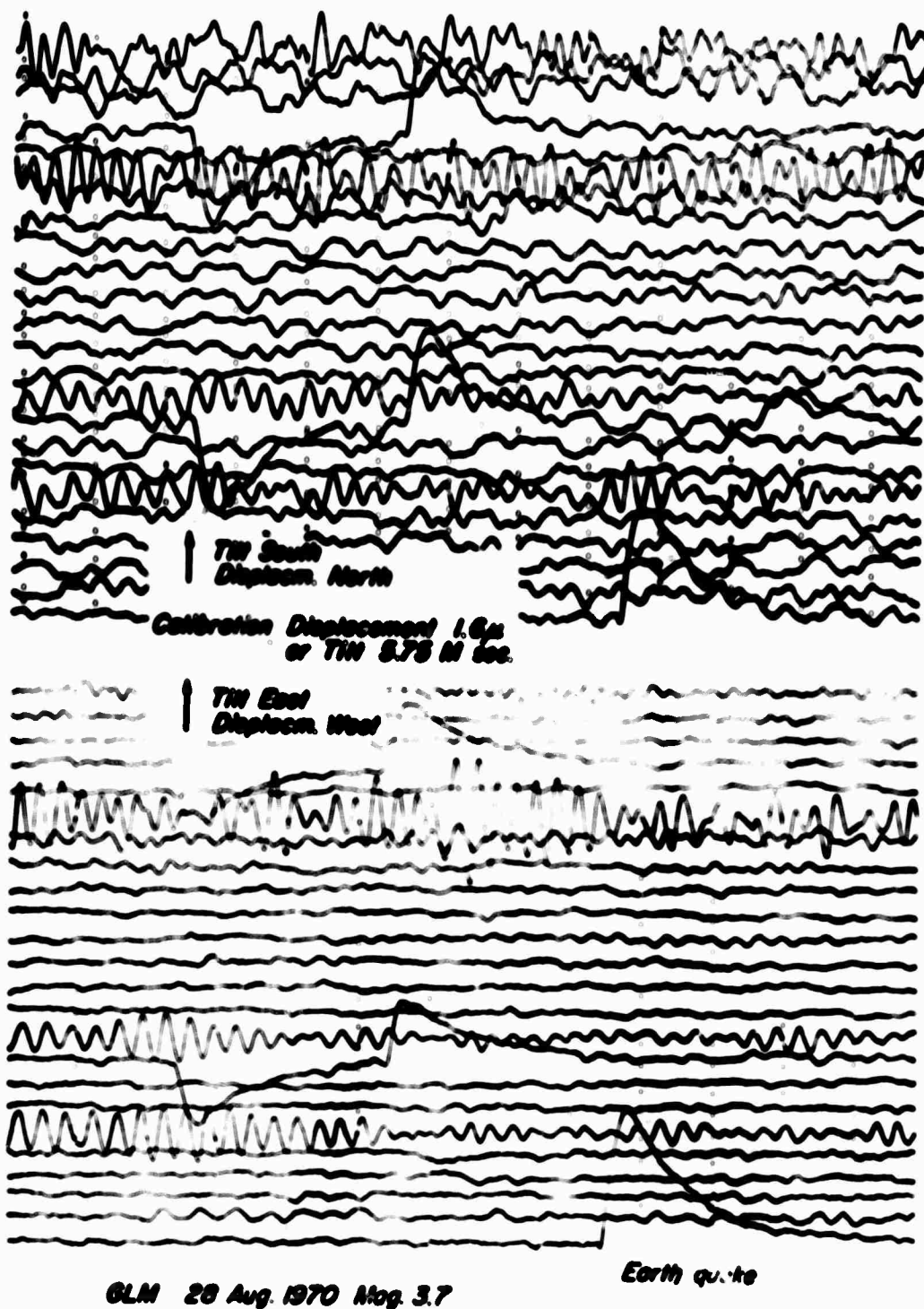


Fig. 14 GLM, 28 August, 1970, tilt records, compare with Figure 15 for the same quake.



**Fig. 15.** GLM, 28 August, 1970, LP horizontal records, compare tilts with Figure 14.

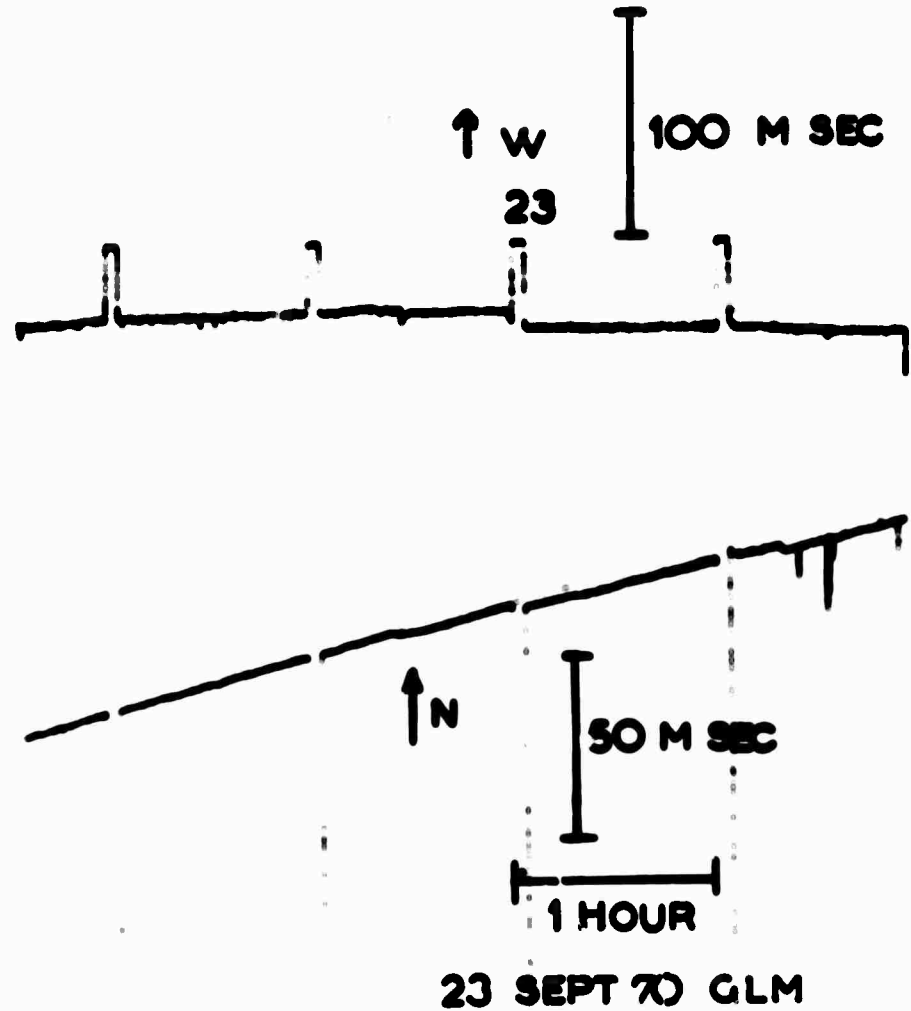


Fig. 16 GLM, 23 September, 1970, tilts, compare with Figure 17.

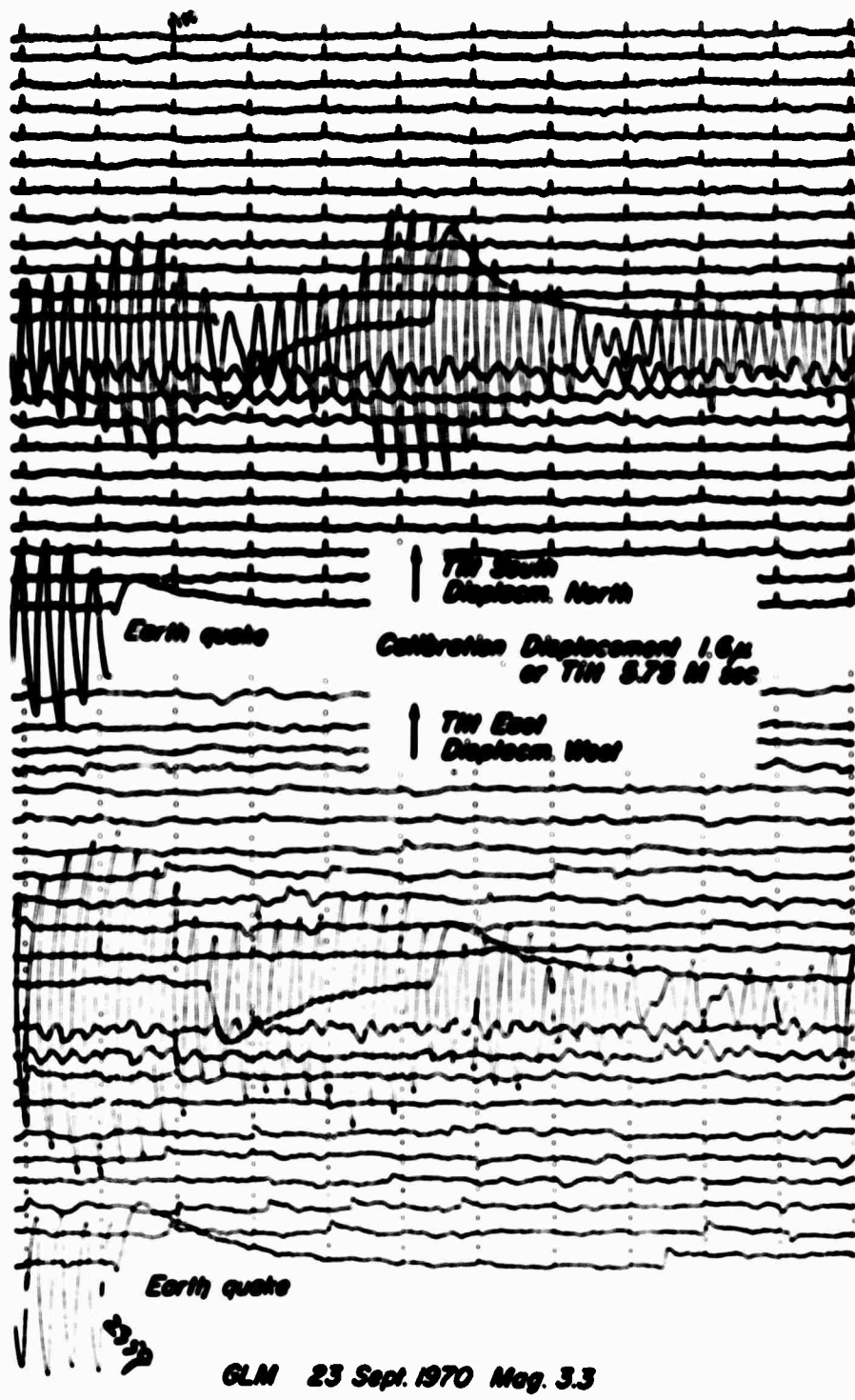


Fig. 17 GLN, 23 September, 1970, LP horizontal records, compare with Figure 16.

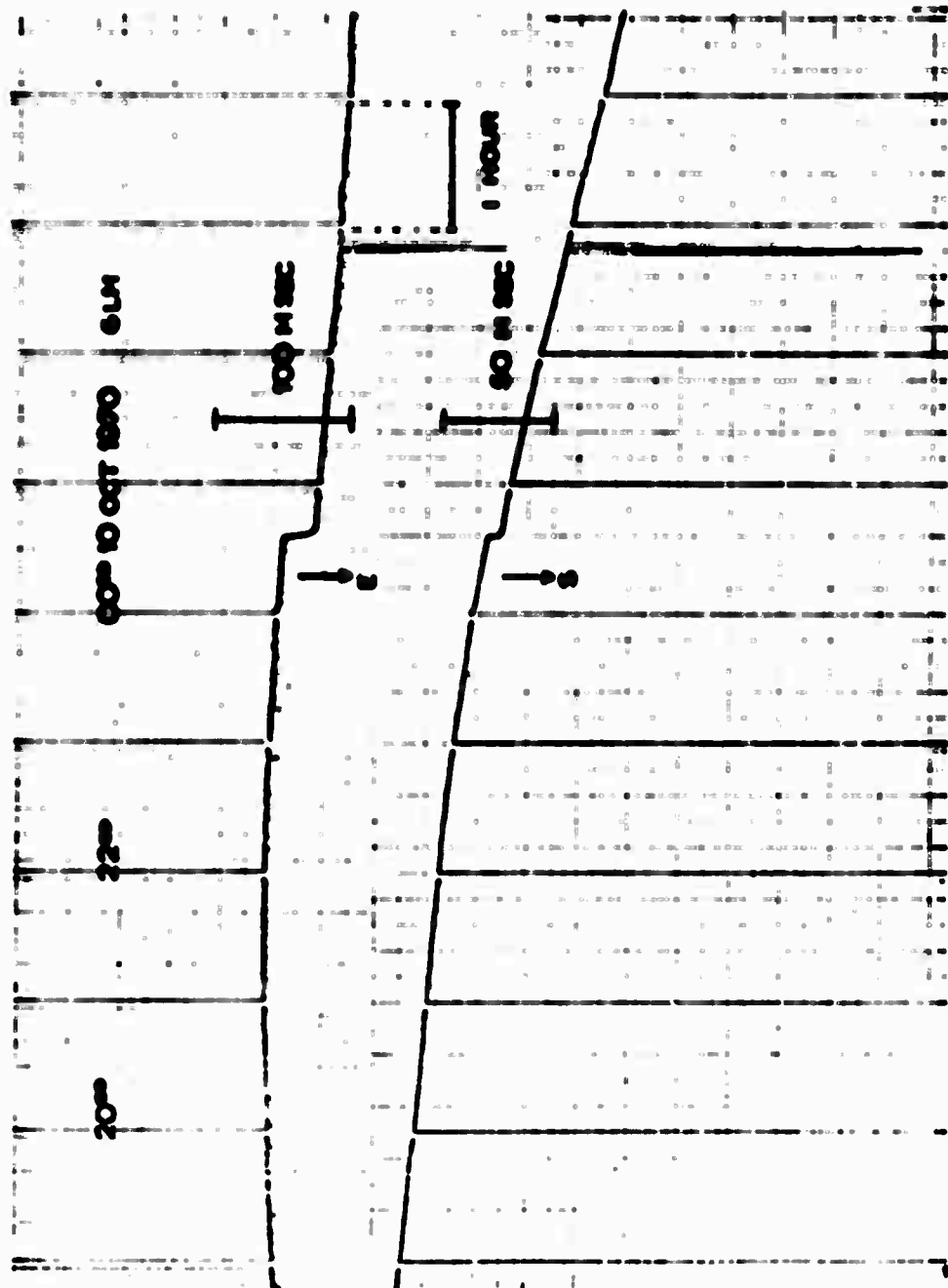
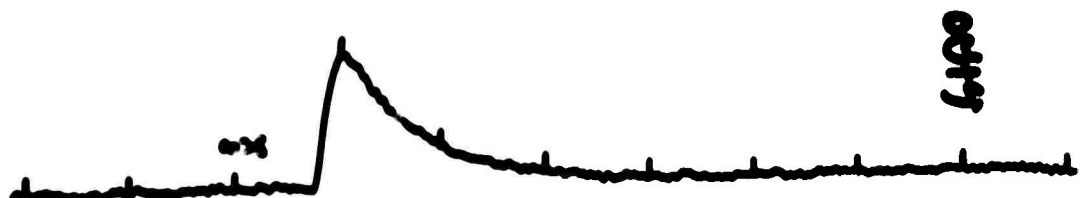


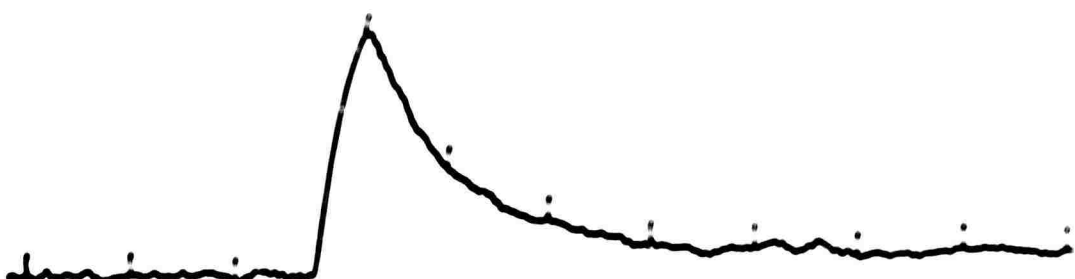
FIG. 18 GLN, 10 October, 1970, tilts, compare with Figure 19.



↑ Till South  
Displacem. North

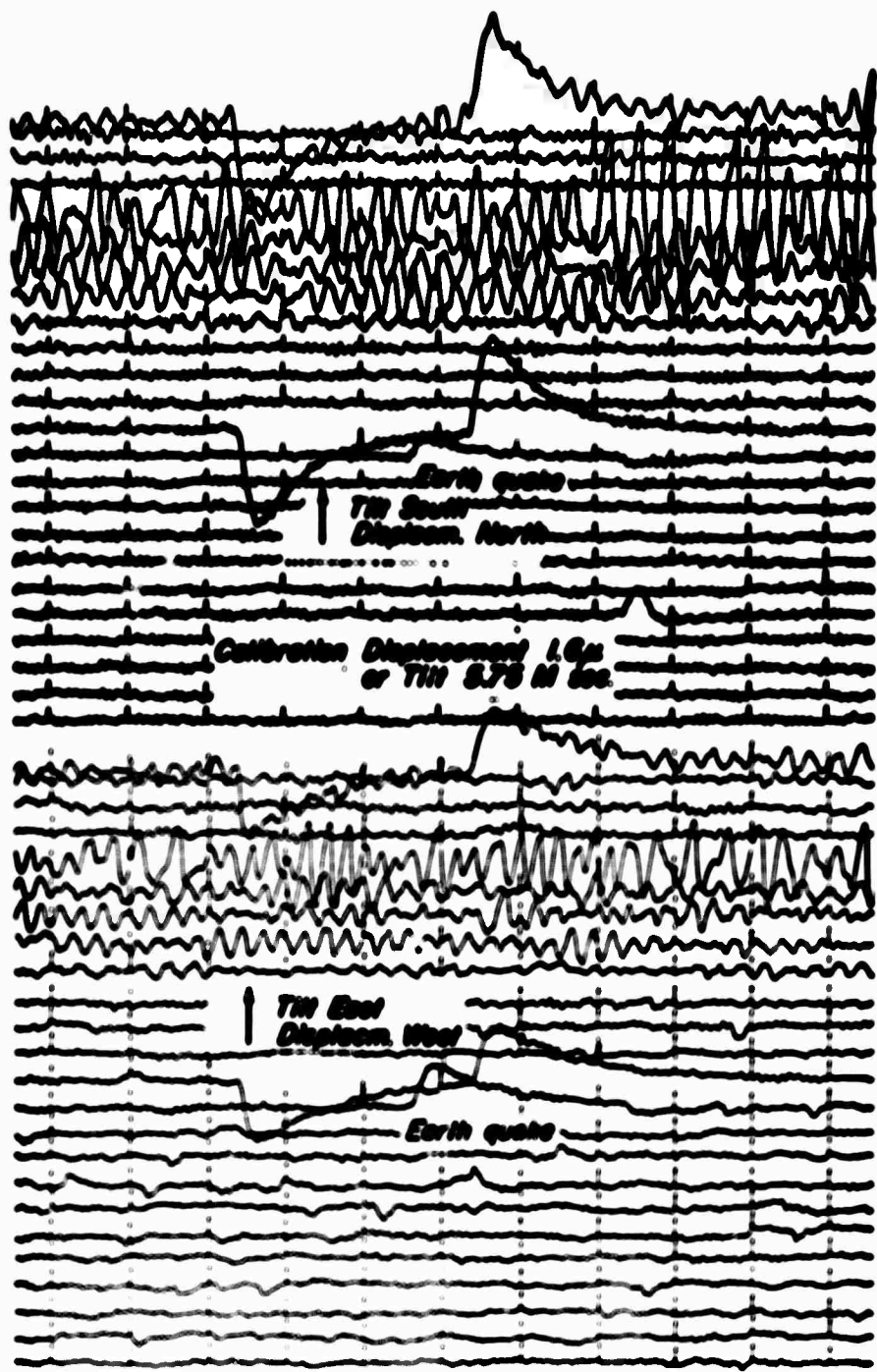
Earthquake

GLM 10 Oct 1970 Mag. 3.2



↑ Till East  
Displacem. West

Fig. 19 GLM, 10 October, 1970, LP horizontal records, compare with Figure 18.



GLM 11 Oct. 1970 Mag. 3.0

Fig. 20 GLM, 11 October 1970, LP horizontal records.

60

840.32

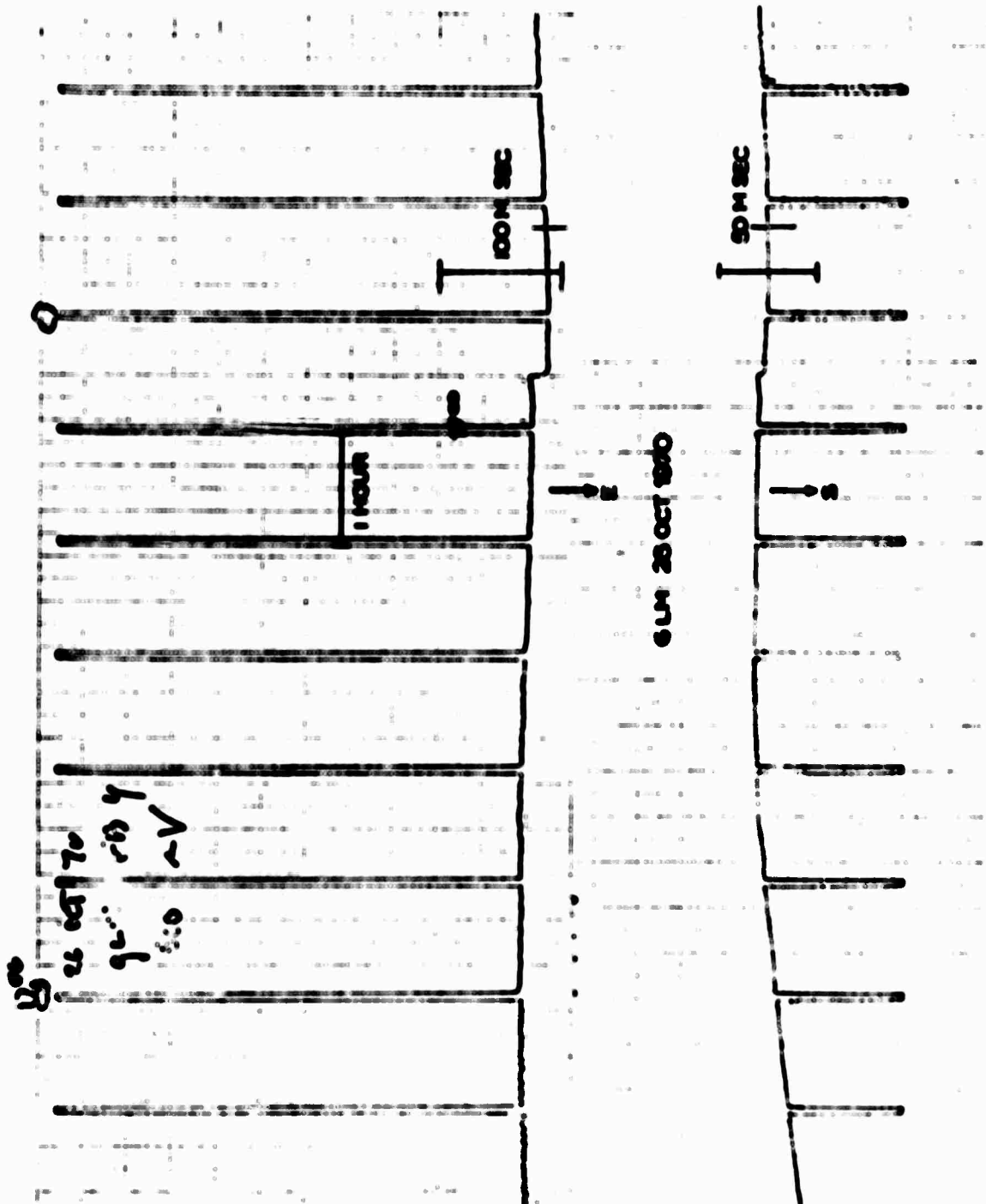
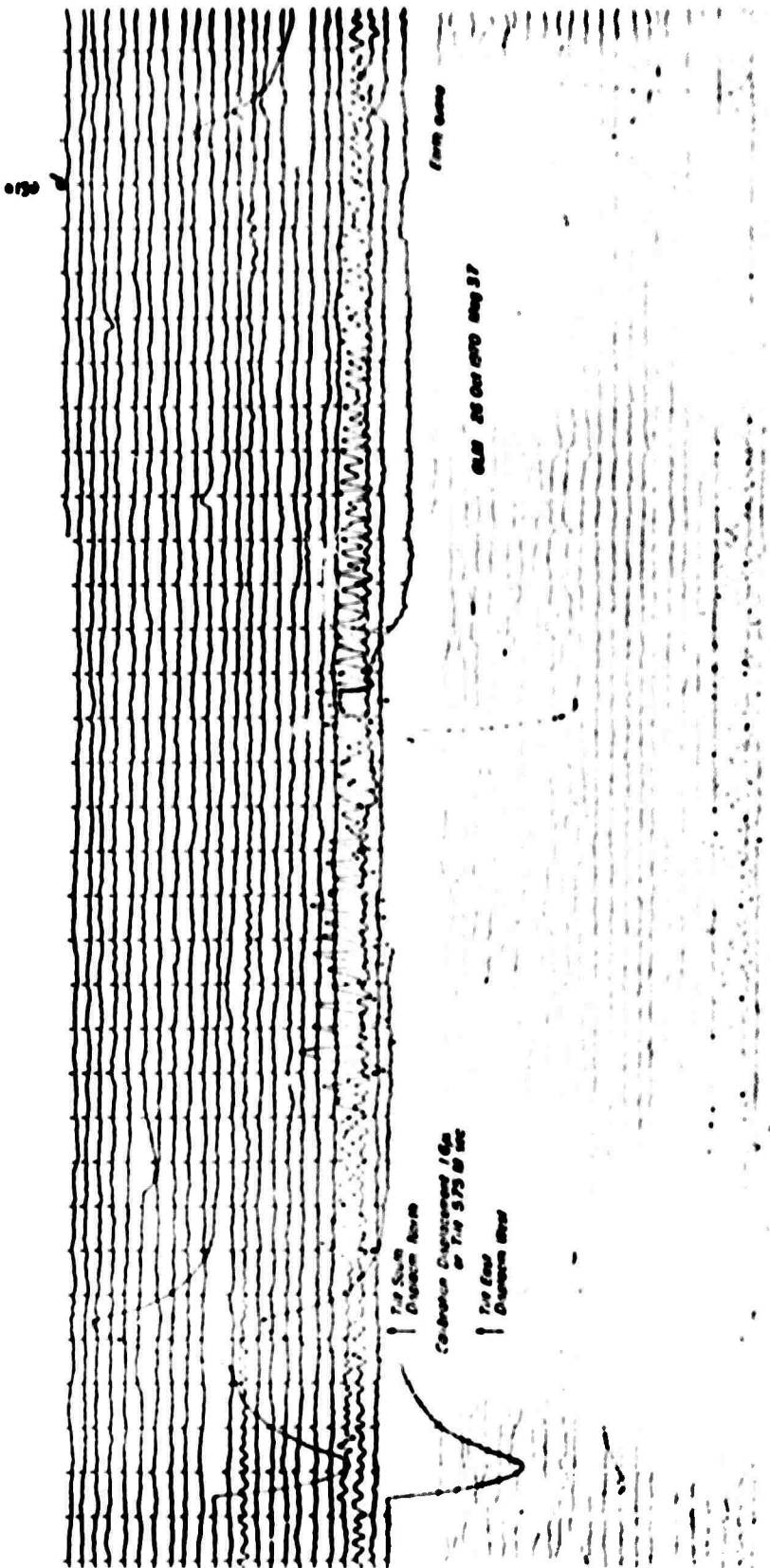
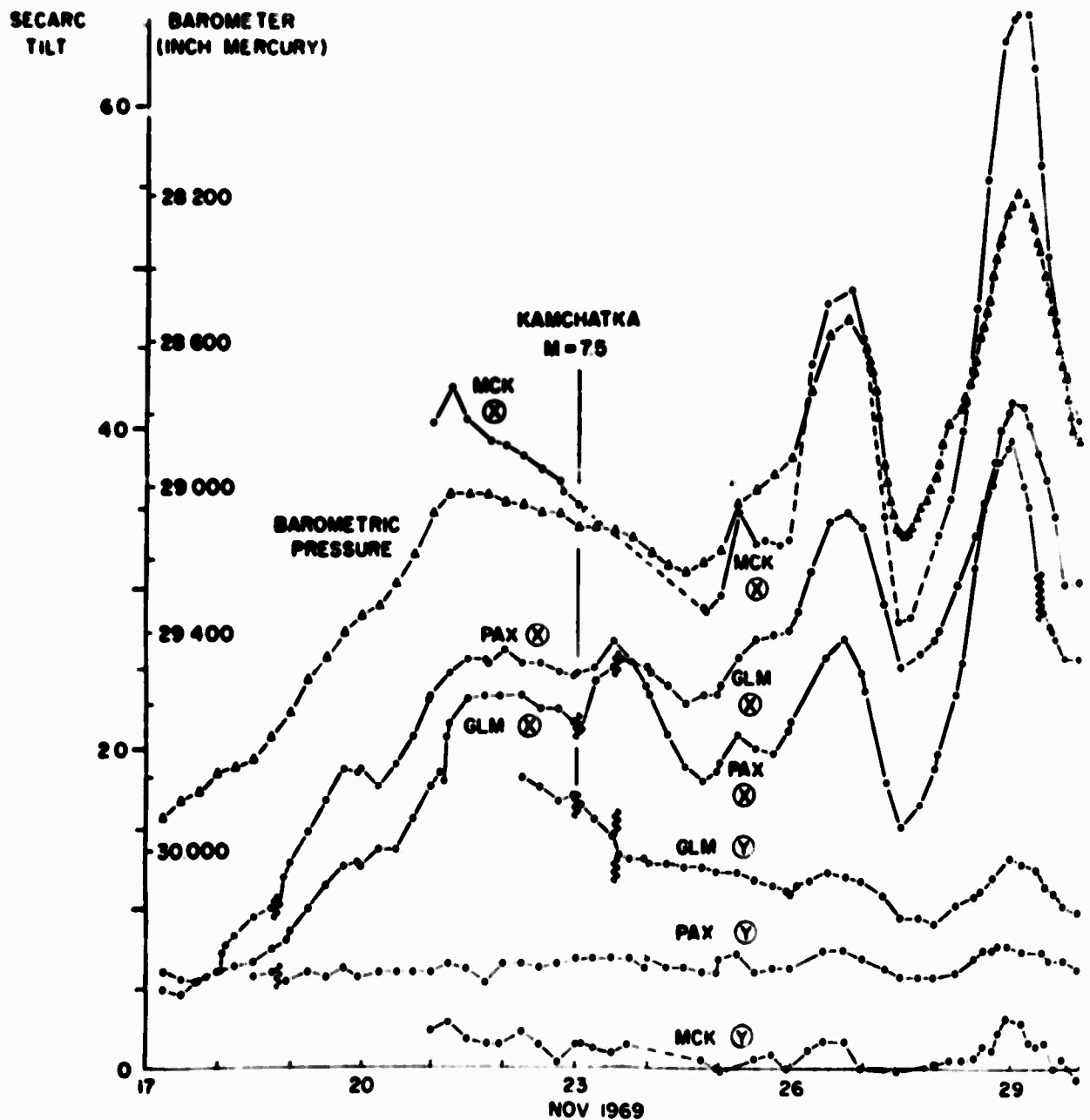


Fig. 21 GLM, 26 October, 1970, tilt records, compare with Figure 22.

GLM 26 OCT 1970

Fig. 22 GLM, 26 October, 1970, LP horizontal records, compare with  
Figure 21.





**Fig. 23** Tilt on the X-component of GLM, PAX, and MCK and Barometric Pressure at the Fairbanks International Airport.

63

FIGURE 23

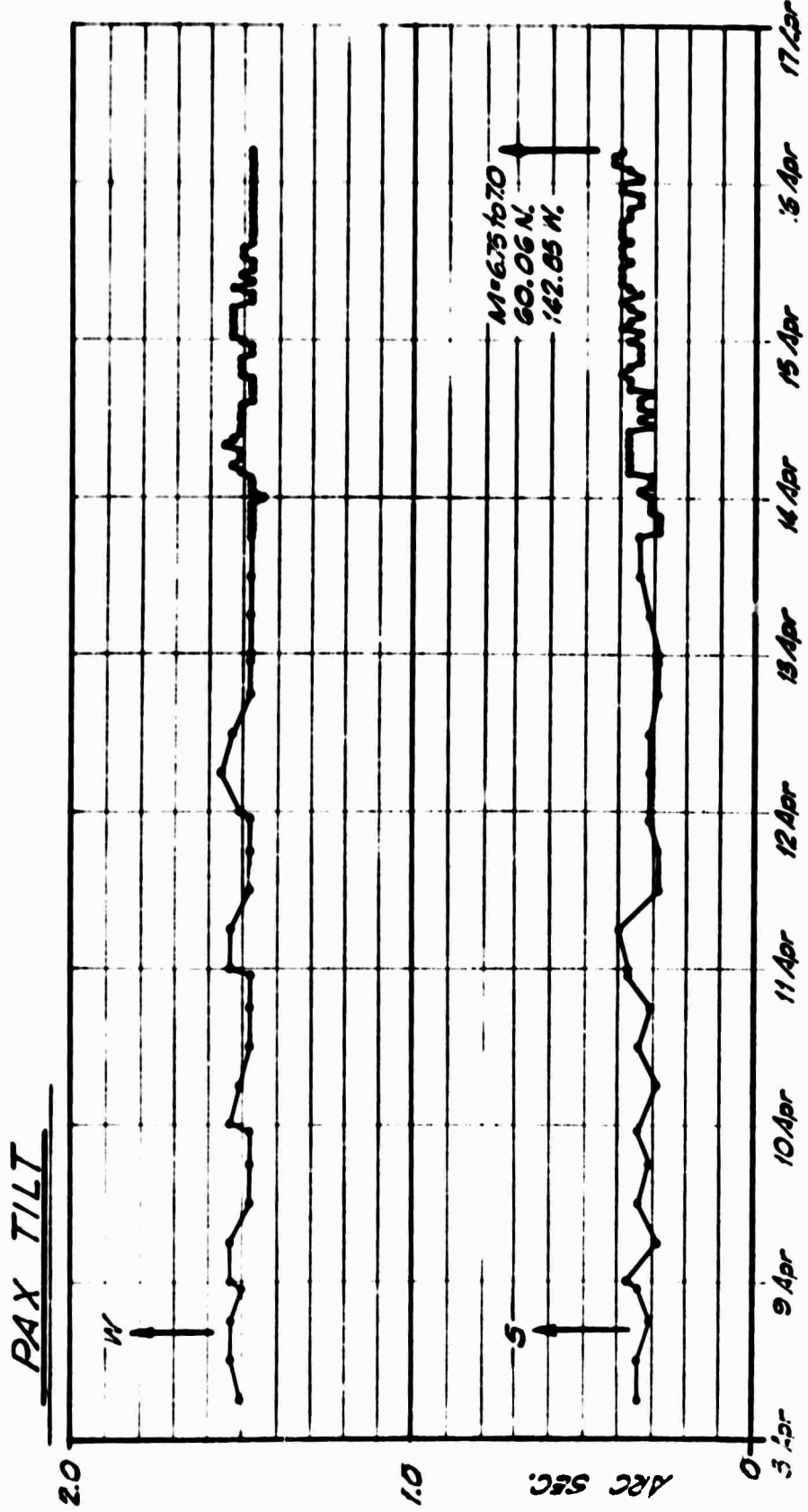
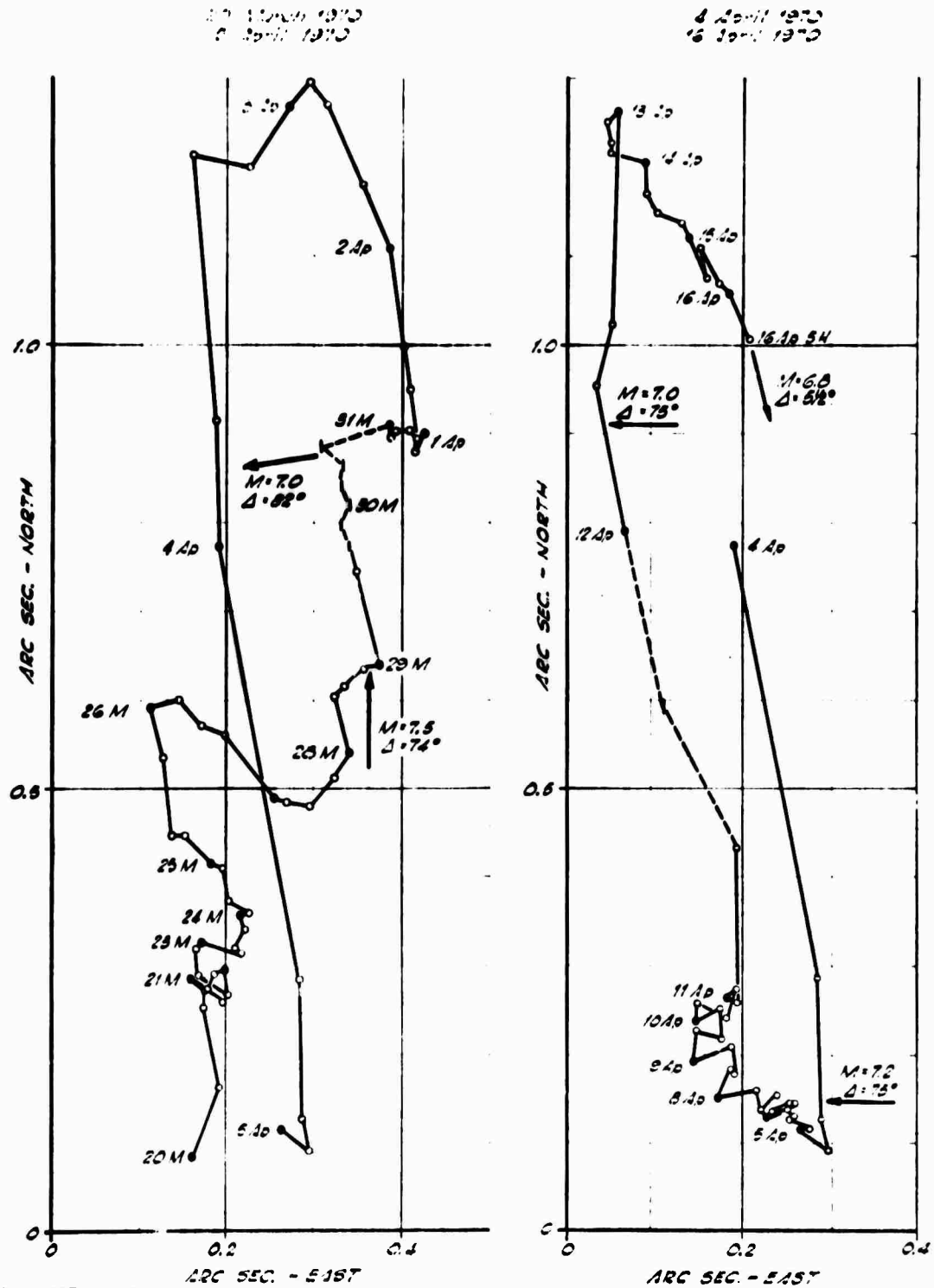


Fig. 24 PAX tilts from 3 April 1970 to 16 April just prior to the Yakataga earthquake.

64

FIGURE 24

### GLM TILT



**Fig. 25** Vector diagram of GLM tilts. Points indicate 6-hourly readings. Note tilt toward the Yakataga area for 3 days, prior to the magnitude 6.8 quake and "S" loop on April 15. Distance to the epicenter is around 650 km.

65

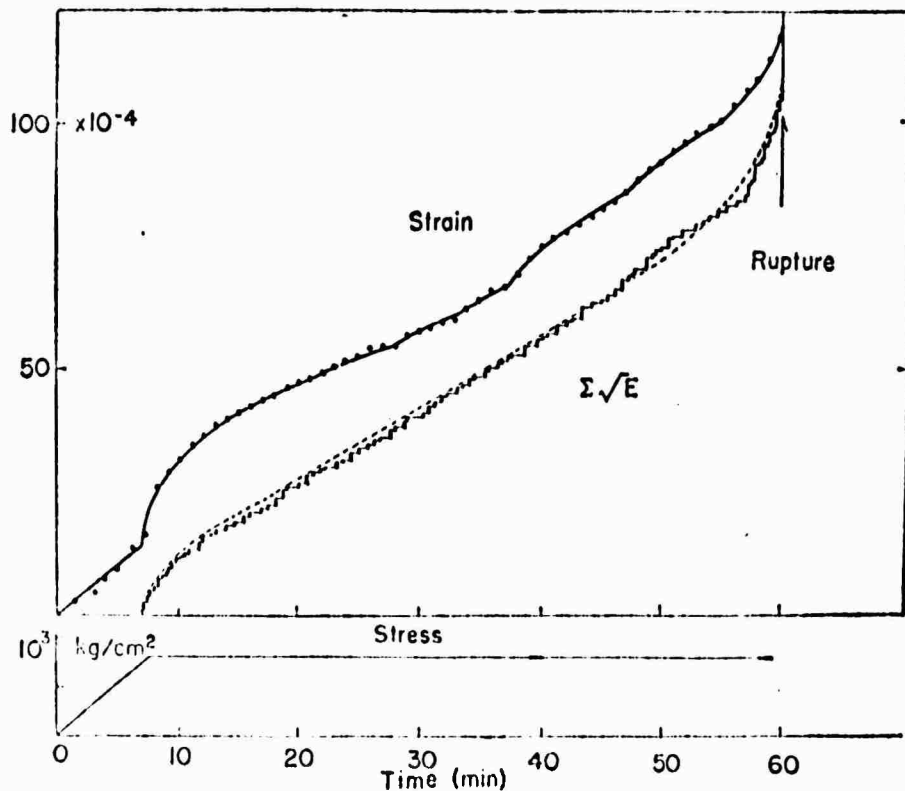


Fig. 26 Laboratory results for strain and strain release by microfractures in granite, for constant stress and temperature, showing pre-monitory, exponential increase prior to failure. (After Watanabe 1963).

- 100 -

M=7 R: 70 km

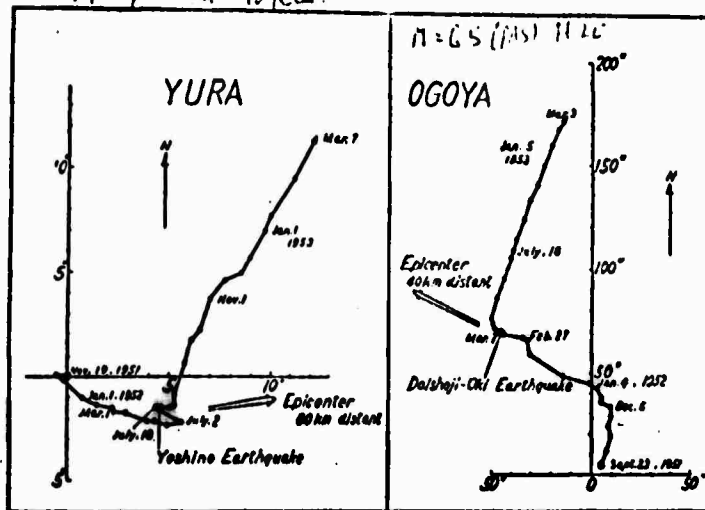


Fig. 3. — Vector diagrams of secular change of ground tilt observed at Yura and Ogoya. Single arrows show the time of occurrence of earthquake and double arrows the direction of epicenter.

from Eiichi Nishimura , 1958

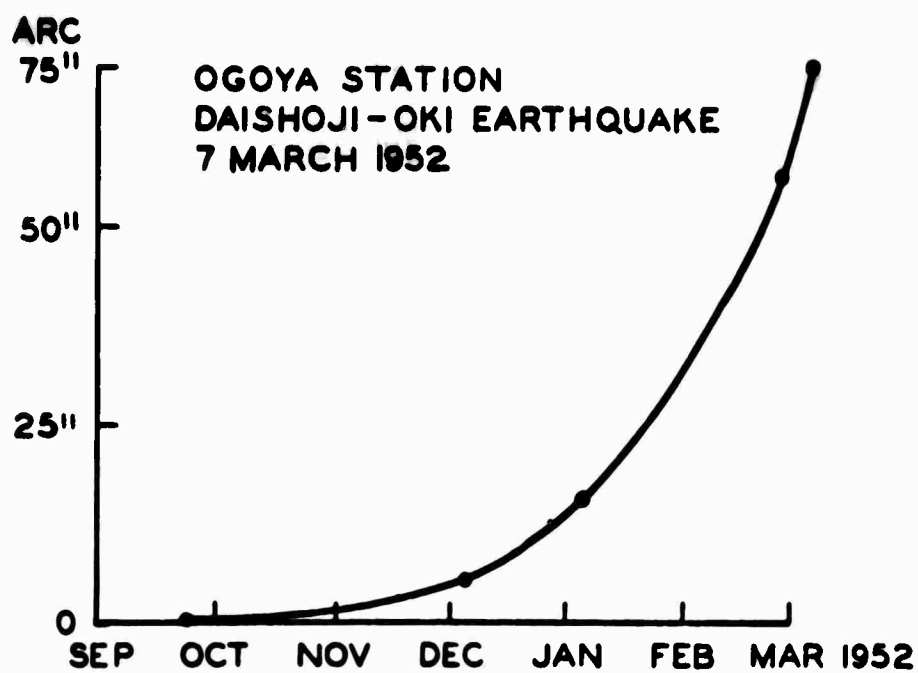


Fig. 27 Tilts prior to the magnitude 6.5 Daishoji-Oki earthquake, 1952.  
a.) original data from Nishimura, 1958.  
b.) tilts towards the epicenter (secular tilts removed from a.)

64

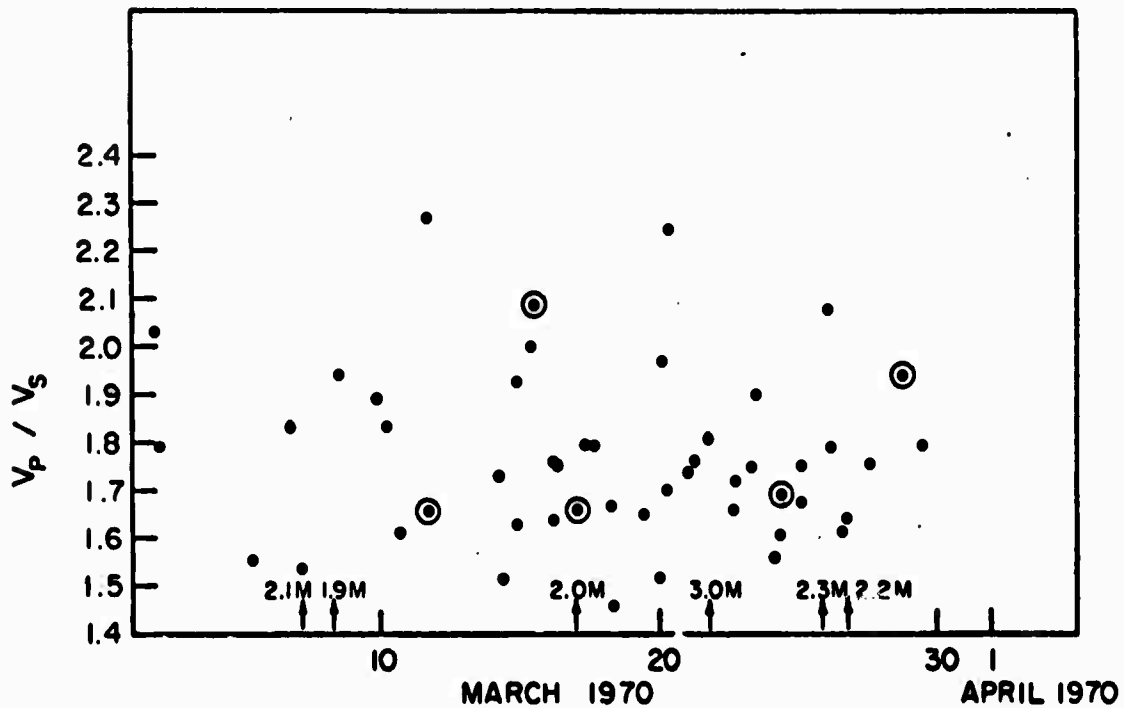


Fig. 28  $V_p/V_s$  in the Fairbanks area, March 1970, dots based on P and S wave arrivals at 3 stations, circled dots on P and S wave arrivals at 4 stations.

**Unclassified**

Security Classification

**DOCUMENT CONTROL DATA - R & D**

(Security classification of title, body of abstract and index/information must be entered when the overall report is classified)

1. ORIGINATING ACTIVITY (Corporate author)  Geophysical Institute University of Alaska College, Alaska		2a. REPORT SECURITY CLASSIFICATION  Unclassified
2b. GROUP		
3. REPORT TITLE  Crustal Deformation Release, Failure and Tilts in Alaska		
4. DESCRIPTIVE NOTES (Type of report and inclusive dates)  Scientific....Final		
5. AUTHOR(S) (First name, middle initial, last name)  Eduard Berg		
6. REPORT DATE  January 1971	7a. TOTAL NO. OF PAGES  75	7b. NO. OF REFS  47
8a. CONTRACT OR GRANT NO.  F44620-70-C-0031	8b. ORIGINATOR'S REPORT NUMBER(S)	
8c. PROJECT NO.  AO 292-75	8d. OTHER REPORT NO(S) (Any other numbers that may be assigned this report)	
8e. 62701D d.		
10. DISTRIBUTION STATEMENT  This report has been approved for public release and sale; its distribution is unlimited.		
11. SUPPLEMENTARY NOTES  TECH, OTHER	12. SPONSORING MILITARY ACTIVITY  AF Office of Scientific Research (NPG) 1400 Wilson Boulevard Arlington, Virginia 22209	
13. ABSTRACT  This report covers the effort during a one year period from the end of 1969 to the end of 1970, supported by AFOSR. The main purpose of the contract was to gain insight into the crustal failure mechanism and the associated source phenomenon in Alaska. This effort includes the operation of the short-period telemetry network and the three long- period borehole installations used for the measurements of crustal tilts.  Through the telemetry system there is now on hand an almost complete record on the seismicity of Central Alaska, covering a total of four years, and of much higher accuracy than was hitherto available.  The operation of the borehole long-period seismometer has revealed tilts associat- ed with earthquakes as small as magnitude 3, which are consistent with the tectonic stress axis, but do not seem to conform to elastic fault dislocation models. Tilt amplitude reductions with distance R is of the form $A \text{ (in sec/arc)} = 10^{M-4.1} \times R^{-1}$ and velocities of tilt propagation are in the range 2.1 to 2.8 km/sec for near earthquakes (focal point to station) and up to 3.3 km/sec for teleseisms. In view of the discrep- ancies with elastic dislocation theory, a surface or crustal type propagation is suggested.  Analysis of literature suggests that Russian observations of the Vp/Vs ratio, diminishing by about 0.1 prior to larger earthquakes, can be explained by the decrease in Vp/Vs ratio due to micro-fracturing (observed in the laboratory) and theoretical as well as experimental work on Vp/Vs changed as a function of porosity. However, so far we have been unable to observe such effects in the Fairbanks, Alaska, micro-earthquake area.		

DD FORM NOV. 1473

**Unclassified**

Security Classification